The role of adsorbed proteins in the internalization of polymeric nanoparticles

Luís Manuel de Mendonça Vieira Lopes Tavares
Mestrado em Bioquímica
Departamento de Química e Bioquímica
2015/2016

Orientador
Pedro L. Granja, Professor Associado, Instituto de Ciências Biomédicas Abel Salazar

Co-orientador
Tiago dos Santos, PhD, Instituto de Investigação e Inovação em Saúde da Universidade do Porto

INSTITUTO DE INVESTIGAÇÃO E INOVAÇÃO EM SAÚDE
UNIVERSIDADE DO PORTO

U.PORTO
INSTITUTO DE CIÊNCIAS BIOMÉDICAS ABEL SALAZAR
UNIVERSIDADE DO PORTO

U.PORTO
FACULDADE DE CIÊNCIAS
UNIVERSIDADE DO PORTO

Todas as correções determinadas pelo júri, e só essas, foram efetuadas.

O Presidente do Júri,

Porto, _____/_____/_____

Agradecimentos

Por onde começar. Foram dois anos de mestrado que passaram a correr, concluindo assim esta etapa da minha vida. Em especial, este último ano, em que conheci várias pessoas novas e juntei-me a um grupo de investigação onde acabei por desenvolver este projeto.

Queria começar por agradecer aos meus pais. Obrigado a ambos por ajudarem-me a realizar os meus sonhos, cada um à sua maneira. Obrigado Mãe pela tua preocupação, por dares sempre a tua opinião e tentar que eu seja sempre uma pessoa melhor. Obrigado Pai, por seres uma referência para mim e uma pessoa que eu espero um dia alcançar e ultrapassar, embora noutra área de trabalho, ou quem sabe…

Obrigado aos meus irmãos, em especial à minha irmã, por se preocuparem comigo de forma única. Vamos ver o que o futuro nos reserva.

Obrigado ao resto da minha família, e em especial aos meus avós, por me acompanharem desde o início do meu percurso. Agradeço em especial o vosso carinho e as vossas histórias de vivências passadas.

Quanto aos amigos de faculdade, agradeço-vos a todos mais uma vez por me acompanharem nesta viagem que ainda não terminou. Especialmente, menciono os amigos mais peculiares que merecem uma posição de destaque: João e Filipa (é sempre bom ver-vos pelo i3S); Ana (fugiste para longe, mas voltas sempre!); Marta, Daniela e Ana (sinto muito a vossa falta); Inês, Diogo, Maria, Ângela, Liliana (vocês eram a principal razão pela qual eu fui ao ICBAS muitas vezes!).

Em relação ao grupo Biomaterials for Multistage Drug & Cell Delivery, quero agradecer-te, Pedro, por teres aceite e permitido que eu realizasse a minha tese de mestrado no laboratório. Apesar do percalço inicial, as coisas lá se ajeitaram. Obrigado pelas conversas e apoio ao longo deste ano. Obrigado Tiago, pela paciência e por ensinares-me tudo que aprendi este ano. Por mostrares que uma pessoa consegue fazer ciência de forma relaxada. E mais uma vez obrigado pela paciência!

Reservo também um espaço ao pessoal de Bioengenharia, que rapidamente conheci este ano, obrigado pela vossa companhia e pelos momentos de riso e humor. Tal não teria sido possível senão fosse devido a vocês os três: Mariana, Miguel e Daniel. A vossa dinâmica é incomparável e juntamente com o Manel, fomos os alunos de

mestrado do grupo deste ano. Acredito que cada um de vocês consegue definitivamente concretizar os vossos objetivos.

I also have a special ‘thank you’ for you Adele. You’ve brought a different dimension to the lab and also changed the view I had of Scotland and its people. Thanks for everything you’ve done, I truly appreciate our friendship.

Para terminar quero agradecer às restantes pessoas do grupo e do i3S que ajudaram, de uma maneira ou outra, a tornar memorável a minha experiência no i3S. Aproveito, rapidamente, para agradecer o apoio todo e auxílio que me deste em relação ao Imagestream, Maria, obrigado por esclareceres todas as minhas dúvidas (que foram de um número considerável).

Resumo

A Nanomedicina está-se a tornar numa realidade cada vez mais sólida, graças aos avanços realizados na nanotecnologia, com a criação de soluções e terapias inovadoras para a cura de doenças crónicas. Sabe-se que a "*protein corona*" forma-se quando uma nanopartícula (NP) entra em contacto com meio biológico e esta presença vai afetar como a NP será "vista" por uma célula. Nesta tese, estudou-se o papel de proteínas adsorvidas na internalização de NPs de polistireno. Como seria de esperar, o perfil de internalização das NPs depende do tamanho das mesmas, das proteínas presentes à sua superfície e do tipo de células em estudo. A informação apresentada neste trabalho apoiou a complexidade da influência que a endocitose celular sofre, quando o tamanho das partículas ou as proteínas de soro são alteradas. De forma generalizada, descobriu-se que partículas mais pequenas que apresentam uma corona derivada de 'proprietary blood fraction' (PBF) sofrem uma menor internalização, quando comparadas com partículas de mesmo tamanho em meio sem soro; enquanto nanopartículas de maiores dimensões, apresentam maior internalização, quando comparadas com partículas do mesmo tamanho, nas mesmas condições. Esta tendência verificou-se em todas as linhas celulares, exceto nas linhas de MKN28 (CD44v6 + e CD44v6 -), onde as NPs de maiores dimensões que possuem uma 'corona' derivada do PBF possuem uma internalização semelhante às NPs de tamanho equivalente, incubadas em meio sem soro. Assim, os dados aqui apresentados confirmam a complexidade da endocitose de NPs, quando se altera o tamanho das NPs ou as proteínas do soro. A compreensão do motivo que leva a esta inversão na internalização, poderá levar a um melhor entendimento da endocitose e a possíveis novas técnicas de entrega de fármacos, em nanomedicina.

Palavras-chave

Nanopartículas, polistireno, nanomedicina, nanotecnologia, 'protein corona', proteínas de soro, endocitose.

Abstract

Nanomedicine is becoming a more important and solid reality, thanks to the advancements made in Nanotechnology, with the creation of innovative solutions and therapies for currently untreatable maladies. It is well known that a protein corona is formed when a nanoparticle (NP) is dispersed in a biological medium and its presence will affect how the NP interacts with the cell. In this thesis, the role of adsorbed proteins in the internalization of NPs was studied by incubating polystyrene NPs, with varied sizes, in different types of serum and then the interaction of the previously incubated NPs with different cells types, was assessed. Results showed that the uptake profile of NPs was dependent of the NPs size, the proteins absorbed to their surface, and the type of cells studied. In general terms, results obtained allow to conclude that smaller NPs exhibiting a Proprietary Blood Fraction (PBF)-originated protein corona resulted in lower cell uptake, when compared to equally-sized NPs in serum free medium, while larger NPs presenting the same PBF-originated protein corona resulted in higher uptake, when compared to same-sized NPs in serum free medium. This tendency was verified among all used cell lines, except in the MKN28 (CD44v6 + and CD44v6 -) cell line, where the larger NPs presenting the PBF-originated corona had the same cellular uptake as same-sized NPs in serum free medium. Overall, the data presented here confirms the complexity of NP endocytosis, when size or serum proteins are changed. Understanding the reason for this change in the uptake could lead to a better understanding on the mechanistic of endocytose and, consequently, to possibly new drug delivery techniques in nanomedicine.

Keywords

Nanoparticles, polystyrene, nanomedicine, nanotechnology, protein corona, serum proteins, endocytosis.

Index

List of Figures and Tables

List of Abbreviations

DNA	Deoxyribonucleic Acid
pDNA	Plasmid DNA
FBS	Fetal Bovine Serum
PBF	Proprietary Blood Fraction
HA	Human Albumin
NP	Nanoparticle
PDI	Polydispersity index
SFM	Serum Free Medium
CM	Complete Medium
RFU	Relative Fluorescence Units
FACS	Fluorescence-activated cell sorting
PBS	Phosphate-buffered saline
DMEM	Dulbecco's Modified Eagle's Medium
RPMI	Roswell Park Memorial Institute
DLS	Dynamic Light Scattering
DME	Doppler Micro-electrophoresis

1. Introduction

1.1. Nanotechnology, Nanomedicine, Nanocarriers and Nanoparticles

In recent years, nanotechnology has grown to become a solid concept that spread throughout the world and impacted all sectors of industry, from Bioengineering and Cosmetics to Energy and Medicine.[1, 2] This term can be defined as the fabrication of new materials and systems with nanoscale dimensions between 1 and 100 nm.[3] In the metric scale, a nanometer is one-billionth of a meter. As a comparative example, the diameter of a ribosome is 20-30 nm and the radius of the DNA structure 1 nm.

Nanomedicine is the use of nanotechnology to develop new approaches, improvements and new therapies in healthcare.[1, 4] New approaches include polymer therapeutics, like polymer-drug conjugates, polymeric drugs or block copolymer micelles.[5] The interest of using polymers in drug delivery and gene therapy relies in their potential of functionalization, its macromolecular synthesis methods, and polymer diversity.[5] All this allows a more direct therapy that focus, at the molecular level, on the unhealthy cells, instead of the healthy ones.

Among the different polymeric structures available, the most studied strategy in nanomedicine is still based in the use of nanoparticles. In a broader sense, nanoparticles can be divided as nanospheres and nanocapsules, both implying distinct preparation methods. While nanospheres consist a polymeric system in which the drug is dispersed in the bulk polymer, nanocapsules are vesicular systems in which the drug is confined to an aqueous or oily cavity surrounded by a polymeric membrane.[6]

Albanese *et al.* revised and discussed the evolution of NPs.[7] The first generation of NPs addressed biocompatibility and toxicity of nanomaterials through material design, especially when dealing with nonbiodegradable particles (like polystyrene, polyacrylamide, and polyacrylate particles).[8] These systems were designed in such a way as to ensure that particles exhibited rapid and efficient clearance, to avoid accumulation and tissue distribution at toxic levels.[9] The second generation of NPs focused at optimizing surface chemistry, taking into consideration stability, stealth, and targeting capabilities of the NPs. The third and current generation of NPs embraced the idea of dynamic ‘smart nanomedicine’ with environmentally-

responsive systems or even prodrugs to improve targeting mechanisms and theranostics abilities, i.e., the combination of therapy and diagnosis.

It is currently widely accepted that for a nanocarrier to be successful, it must satisfy a number of design criteria, such as drug loading capacity, triggered or appropriate release, optimized biocirculation (stealth), serum/plasma stability, lack of toxicity, targeting ability, lack of immunogenicity, adequate cell uptake and be noncumulative.[10] Although several combinations of nanoparticulate formulations have been developed, in the specific case of cancer the perfect nanocarrier platform capable of targeting a large range of cancer cells, with minimum side effects, is still out of reach, but much closer than it was several years ago, with several new approaches undergoing clinical trials.[11, 12]

1.2. Nanomedicine in Cancer

Neoplastic cells are peculiar abnormal cells with several accumulated genetic mutations in key genes, which altered their behavior and morphology, leading to uncontrollable cell proliferation and an absence of cell death, and eventually to the formation of a tumor and progressing into cancer, afterwards. Hanahan and Weinberg proposed six hallmarks that constitute an organizing principle and helps understand the incredible diversity of neoplastic diseases. The following capabilities characterize most cancers: the ability to evade apoptosis; an acquired insensitivity to anti-growth suppressors; a sustained proliferation signal; the activation of invasion and metastasis; the limitless replicative potential; and the ability to sustain angiogenesis.[13] The acquisition of these capabilities is possible due to the cell's genome instability and mutations in genes that regulate the above mentioned abilities and a tumor-promoting inflammation, which aids in the creation of an adequate microenvironment for tumor-proliferation.[14] They also suggested two additional new hallmarks, probably involved in the pathogenesis of some or even all cancers: the capacity to reprogram cellular metabolism in order to effectively support neoplastic proliferation; and the ability to evade the immune system's agents.[14] Such diversity, combined with its potential to develop resistance to current therapies, is what makes so difficult to treat it.[15] Understandably, cancer is the second worldwide cause of death, exceeded only by cardiovascular diseases.[16]

The selection of an anti-cancer therapy depends on the type of cancer, its location and grade diagnosed. Well localized solid tumors are normally treated with

surgery, and mostly complemented with chemotherapy and/or radiotherapy. Such treatments also have a negative impact on healthy cells, causing their death. To overcome those relevant drawbacks, and especially the side-effects on healthy cells, new and more targeted approaches have been developed and several targeted treatments are already clinically available, involving antibodies or drugs, used to treat specific types of cancer, such as for example: Trastuzumab (HER-2 positive metastatic breast cancer), Rituximab (diffuse large B cell non-Hodgekin's lymphoma), or Geftinib (non-small cell lung cancer), among others approved by the FDA and EMA.[17]

Nanomedicine has also been contributing with new drug delivery systems, providing promising anti-cancer therapies and/or improving chemotherapy. Nanocarriers are claimed to be able to accumulate preferably in tumors, avoiding healthy tissues, achieving cytotoxic concentration several-fold higher, and with reduced toxicity for the rest of the body, compared with free drugs.[18-20] The nanocarrier also protects the agent from degradation, reduces renal clearance and increases its half-life in the bloodstream, allowing for a smaller dosage of the drug to be used.[20] Additionally, the defective vasculature surrounding the tumors also allows passive accumulation of nanocarriers in tumor tissues, releasing the chemotherapeutic agents in its vicinity – the so called enhanced permeability and retention (EPR) effect.[21]

Current anti-cancer therapies in the clinics which use nanoparticulate systems include some of the following drugs: Taxol®, micelles containing paclitaxel which are used as part of first-line chemotherapy (approved on 1992, FDA); Oncaspar®, a polymer-protein conjugate used on acute lymphoblastic leukemia (1994, FDA and 2014, EMA); and Abraxane®, albumin nanoparticles bound with paclitaxel used on metastatic adenocarcinomas of pancreas and metastatic breast cancer, among other types of cancer (2005, FDA and 2008, EMA). Several other promising new therapies are also under clinical evaluation.[11]

In summary, the current major focus in this area is focused on developing improved ways to specify the targets of drug delivery carriers, so that these are only internalized by the target cells. However, the whole field still requires a deeper and better understanding on the mechanisms of endocytosis to improve its efficacy.[22]

1.3. Nanoparticles and Cellular Uptake

Beyond this point, the different endocytic mechanisms, the NP physicochemical properties and their effects on the uptake will be discussed, followed by an introduction about the protein corona.

1.3.1. Endocytic Mechanisms

Here, some aspects and considerations of the unique and different uptake pathways are summarized.

Phagocytosis is a well characterized pathway, unique to specialized mammalian cells such as neutrophils, monocytes and macrophages. These cells are part of the immune system whose role is to internalize and digest cellular debris and pathogens, being one of the most important physiological line of our organism's defense. When a pathogen is recognized by specific cell surface receptors signaling cascades, mediated by Rho-family GTPases, are induced and trigger polymerization of actin membrane protrusions at the ingestion site.[23]

Clathrin-mediated endocytosis (CME) involves specific receptors that recognize and internalize cargo into "coated pits", constituted by an assembly of cytosolic proteins, clathrin, which is the main assembly unit. These coated pits invaginate and close off to form early endosomes, which will later fuse with lysosomes.[24-26] Typical sizes of coated pits range from 60-200 nm diameter.[27]

Caveolae-mediated endocytosis happens as the result of the clustering of lipid raft components and the interaction of different proteins, especially caveolin, with the cellular membrane. The final product is the caveolae, flask-shaped invaginations, which are very abundant at the surface of endothelial cells. Internalization via this pathway is induced by specific ligands, such as simian virus-40 or cholera toxin. It is also considered to be the predominant pathway of entry for particles bigger than 200 nm.[27-29]

Other internalization pathways have been classified as clathrin- and caveolae-independent endocytosis, which involve other types of cholesterol-rich microdomains on the plasma membrane. These domains, capable of diffusing on the cell surface, are generally known as lipid rafts and have a diameter of 40-50 nm, and are capable of internalizing particles with ~90 nm in diameter.[30-33]

Lastly, micropinocytosis involves the internalization of big areas of the plasma membrane, together with large amounts of fluid. Since uncoated vesicles can be bigger than coated ones, this endocytic pathway allows the uptake of larger objects (>150 nm). Actin rearrangement, together with the stimulation of Rho-family GTPases, are a crucial part of this mechanism.[34, 35]

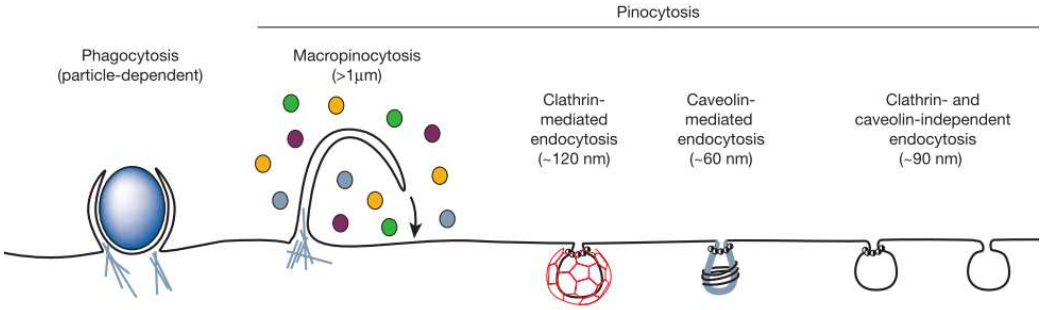

Figure 1- Multiple endocytic portals that allow entrance into the cell (adapted from Conner et al).[32]

1.3.2. Influence of Particle Size, Shape and Surface Chemistry

Particle size can be controlled through multiple material selection parameters (e. g., surfactant used, polymer type, and concentrations) and through various fabrication methods (e. g., type, nozzle diameter, flow rate, control agent, monomer, initiator, polymerization, and emulsion type.[12, 36, 37] Nanoparticle size affects both the uptake efficiency and kinetics, the internalization mechanism, the subcellular distribution, the functions of circulation, targeting (interaction with the cells), degradation, toxicity and opsonization. According to some works, the nanoparticle size will even influence some of the corona's characteristics, like thickness, composition and protein activity, which will modulate their cellular interactions. [37-42]

The route of NP uptake, which can be affected by the cell membrane-nanoparticle interaction, may be defined by two successive stages: the adhesion process of the particle to the cell membrane and an internalization process.[43] A size-dependent uptake has been observed in different cell lines, independently of the particle material composition.[7, 38, 40, 43-48] Hoekstra *et al.* used a range of fluorescent latex beads of defined sizes (50-1000 nm) to investigate the effect of NP size in non-phagocytic B16 cells and verified that the internalization of NPs <200 nm was observed to involve Clathrin-coated pits. But when the size was increased, caveolae-mediated

internalization became more apparent and predominant, especially in the entry route for 500 nm particles.[27] Rafailovich *et al.* reported that 45 nm Au NPs entered cells via clathrin-mediated endocytosis, while the smaller 13 nm particles went mostly through phagocytosis.[49] Chan and coworkers studied the uptake of Au NPs (14-100 nm) in HeLa cells and reported maximum uptake for 50 nm particle.[50] Kulkarni *et al*. studied the uptake of PS NPs (size range 25-500 nm) for drug delivery across the blood-brain barrier. NPs with diameters <200 nm were taken up by Caco-2, a human colon adenocarcinoma cell line, and MDCK, Madin-Derbey canine kidney cells. The 100 nm particles resulted in maximum uptake, in Caco-2 and MDCK cell lines, while the 500 nm were poorly internalized. Smaller NPs were cleared by the reticuloendothelial system (RES), which reduces the uptake efficiency due to the reduced circulation time (<100 nm). In addition, smaller NPs do not have a small enough surface area to meet the energy requirements for the membrane bending process, which occurs before endocytosis. It is suggested that 100-200 nm particles are internalized by receptor-mediated endocytosis while larger particles, are taken up through phagocytosis.[46] Nanoparticles with a diameter <100 nm are able to penetrate into tumors, through its leaky vasculature (EPR effect). But within the tumor microenvironment, the EPR effect is mitigated most of the times due to the presence of host stromal cells, which contain cancer-associated fibroblasts that can promote cancer initiation, angiogenesis and metastases.[51]

Overall, when comparing several works, it can be noticed that there is usually an optimal size for an efficient uptake of NPs and this critical size will vary depending on the cell type used and surface properties of the NPs. It seems also evident that, due to the great variation found in the literature regarding “ideal” nanoparticle size, it is challenging to correlate beyond any doubt a particular cellular response with NP size.[38] Several studies have presented contrasting results based on the cell line under study, NP material and its surface properties, differing polydispersity values, probe area complexity, among other more specific parameters.[52] In what concerns particle size and its influence on cell uptake the real challenge seems to lies in working through the combinations of potential nano-bio situations and to try and understand how and why certain outcomes are obtained. Guidelines for what particle size might be useful for certain applications in nanomedicine are listed in the following Table 1.

Table 1- Nanoparticle size relative to clearance and applications.

Particle Size (based on Rigid Sphere)	Nanomedicine Applications	Ref
< 10 nm	Fast clearance through extravasation or through urinary system.	*53*
10-20 nm	Detection, imaging, potential to cross blood-brain barrier (BBB).	*54*
20-100 nm	Drug/gene delivery, cancer therapy, sites of inflammation (optimal range to avoid physiological barriers; high circulation potential, reduced hepatic/splenic filtration).	*53-56*
100-200 nm	Drug/gene delivery (high potential for prolonged circulation)	*54*
200 nm-1 µm	Generally cleared by the spleen.	*56*
>1 µm	Normally opsonized and accumulate in liver and spleen, being cleared from circulation almost immediately.	*53, 54*

A particle's shape also influences the adhesion and transport of particles.[47] It can also influence the efficiency of cellular uptake. Nanoparticles of the most various shapes and forms have been made and reported, from nanorods to nanostars, and from filomicelles to nano-bullets.[57]

Spherical nanoparticulate systems are the most commonly studied nanoparticles, both *in vivo* and *in vitro*, due to several advantages that can be grouped in the following four areas: a versatile and modifiable platform to build upon, a high surface-to-volume ratio, shape and size, and unique optical properties.[58] Also, nanocarriers have been mostly designed as spheres simply because of the ease of manufacture, restricting information on the influence of nanoparticle shape on biocirculation.[59, 60]

Assymetrical and nonspherical polymeric nanoarchitectures have been considered in nanomedicine as a way to perform complex tasks and mimic complex biological systems. [61-63] The usage of differently shaped-particles allows unique interactions with complicated biological systems in adhesion, transport, drug delivery/release, circulation time, and biodistribution.[64] Nanomedicine applications, such as sensing, self-assembling, tissue engineering, immunoengineering, and therapeutic and diagnostic delivery will benefit from the existence of these nanoparticles. [12, 65]

In a mini-review, Tao et al. described several top-down engineering methods to produce nanoparticles with a certain shape: particle replication in nonwetting template (PRINT®) methods, stretching of polystyrene particles, step flash imprint lithography

polyethylene glycol diacrylate (S-FIL PEGDA) particles, and template-induced printing of nanoparticles.[66] Different shaped nanoparticles, other than spheres, include: rectangular disks, rods, worms, oblate elipses, elliptical disks, needles, plateloids and circular disks, to name a few.[12, 66] Such unique morphologies, with complex surfaces, could allow a more controlled targeted delivery based on the potential for variable ligand presentation that could originate. However, the surface-cell interactions will be more difficult to understand, considering the resulting nano-biointerface and the different presentations a particle could be introduced to a cell upon uptake.[12, 66] For example, a rod-shaped particle can be presented on its short axis (or rocket mode) or long axis (submarine mode), which can lead to two very different cellular responses.[12, 67]

Gratton *et al*. fabricated micrometer-sized particles in various shapes with the PRINT® technique. The research focused on whether the particle morphology affected cellular internalization and intracellular trafficking by HeLa cells. It was found that rod-like particles with a high aspect ratio had increased internalization rates, almost four times faster than more symmetric cylindrical low-aspect-ratio particles.[68]

Discher *et al*. reported the persistent circulation of soft filamentous or worm-like micelles of approximately 1 week in mice and rats, proving the importance of nanoparticle shape.[69] The circulation time of filomicelles in the human body was estimated to be up to 1 month.[69, 70] Polymeric fillomicelles have nanoscale diameters ranging from 22-60 nm tuned by the polymer molecular weight and with contour length controlled by repeated extrusion of worms through nanoporous filters.[71] The filomicelles were constituted by a hydrophilic PEG corona and a hydrophobic core of inert polythethylene or biodegradable polycaprolactone. Unlike filomicelles, PEGylated spherical stealth vesicles (presenting the same surface characteristics as the filomicelles) injected at the same dose were cleared within 2 days, firmly establishing a correlation between the nanoparticle shape and circulation time.[10] Furthermore, filomicelles with a contour length of approximately 8 μm had the longest circulation time, while longer particles quickly fragmented, following injection in mice, indicating a relation between filomicelles contour length and circulation time.[69]

Concerning other cylindrical shapes, PEGylated gold nanorods were observed to have reduced clearance, with longer circulation times when comparing to their spherical counterparts.[72] Zhou *et al*. reported similar results using nanorods with a hydrophobic biodegradable camptothecin core and a hydrophilic coat constituted by linear PEG and dendritic polylysine. These rods were found to have prolonged

circulation times, high cellular uptake and increased accumulation in mice tumors compared with the spherical nanoparticles.[73]

Other unusual shaped-nanoparticles include Janus particles, “dumbbells”, “snowmen”, “rattles”, “raspberries”, “stars”, “flowers” or even “sea urchins”. These surprising nanoparticles have peculiar shapes which affects their biological activity and the cellular and their *in vivo* fate.[38, 74]

Janus nanoparticles are asymmetric spheres with two physically or chemically distinct surfaces. Janus nanoparticles are named after the roman god Janus whose head is represented with two opposite faces. Several combinations of multicomponent hetero-nanostructures have been made, including either purely organic or inorganic particles, as well as composite organic-inorganic compounds. As such, they have attracted increased interest in the area of biomedical applications, especially for theranostics and treatments.[75] A number of published articles focus on the preparations of such particles.[76-79] For instance, Shao *et al*. engineered multifunctional Janus nanocomposites, constituted by a metallic head of magnetic Fe_3O_4 and a body of mesoporous SiO2 containing DOX (doxorubicin). These “nano-bullets” (M-MSNs-DOX) possessed superior magnetic properties, a finer controlled aspect-ratio and defined abundance in pore structures. M-MSN-DOX was tested on subcutaneous and orthotropic liver tumor models in mice, it was reported that the proposed Janus nano-bullets, when under the influence of a magnetic field, had an increased endocytosis by cancer cells and were able to suppress tumor growth and significantly reduced systematic toxicity, since pH-promoted DOX release only happens in the acidic environment found in these cells. This study is an example of an intriguing targeting strategy for safe and efficient liver cancer treatment based on a novel bullet-shaped Janus NP.[80]

Considering all published literature, it seems clear that the factors discussed previously have a determining influence in a nanoparticle’s behavior *in vivo* and *in vitro* (especially in cellular uptake). However, the current conflictive nature of the evidence obtained make it premature to draw detailed and absolute conclusions on the effect of the several parameters, namely concerning particle shape. Further work needs be dedicated to investigating the effects of size, shape, charge, surface characteristics, rigidity, protein corona composition, nanoparticle concentration, as well as cell types, endocytosis mechanisms, medium, flow velocity, and others factors. A better understanding on how each parameter independently affects cellular uptake and

nanoparticle behavior, and, at the same time, the complexity of their interplay is required.

In the context of the present work, it is also reasonable to consider that the corona will also be influenced by the size of the nanoparticles. According to Cedervall's results, there was a distinct difference in the degree of protein surface coverage of the NPs depending on their size, with a larger degree of protein coverage on the larger particles. When decreasing the NP size, from 200 to 70 nm, a suppression of the protein adsorption was observed.[81] Such suppression could be due to the NP's curvature. Klein claimed that the curvature of smaller NPs suppressed the adsorption of certain proteins, mainly those with larger size or less conformationally flexible proteins.[82] Despite all the advantages of using NPs for therapeutic purposes, namely for smart therapeutics or personalized medicine, there is still a small number of FDA or EMA-approved NP-based treatments, drugs and devices.[12] A better understanding of the influence protein corona on the cellular uptake of nanoparticles, and its modulation through different types of serum, may eventually contribute for new achievements in nanomedicine.

1.3.3. Protein Corona

An important aspect to take into consideration when considering the use of nanoparticles is their fate after entering the human body. Nanoparticles, due to their size, are processed and taken into the cell by active, energy-dependent processes. The primary contact between both is mediated by the nanoparticle's surface in the biological medium.[27, 68, 83-85] But when the surface of nanoparticles comes in contact with any biological medium or body fluid, it will be modified by the adsorption of biomolecules such as proteins and lipids, culminating in the formation of a layer of molecules called "protein corona".[40, 81, 86-89] The primary forces for adsorption of proteins on nanoparticles are hydrophobic and electrostatic, so the surface charge will also affect the resulting corona.[90, 91]

The "protein corona" has a dynamic nature since a limited number and specific type of biomolecules will compete for the nanoparticle's surface, resulting in a corona containing a few (mostly) identifiable proteins.[81, 86, 92-96] If the exchange kinetics is slow enough (depending on the coating proteins and the experimental setup), the corona will be biologically relevant and it will be the primary contact with the cells, becoming the nanoparticle's biological identity.[81, 97, 98] In other words, the identity, organization and

lifetime of these proteins adsorbed on the particle's surface affects the way cells will interact with, recognize and process these nanoparticles.[87, 94]

Dawson and Lynch hypothesized that once the nanoparticle is dispersed in any biological fluid, a cell will only "see" the system in which the core nanoparticle is surrounded by a "hard" corona of slowly exchanging proteins, tightly bound, and an outer layer of weakly interacting protein-protein complexes, rapidly exchanging with the proteins present in the environment ("soft" corona).[99-102] Milani *et al.* confirmed this theory through their study of reversible vs. irreversible binding of transferrin to polystyrene nanoparticles.[103] Between the two, the inner hard corona is of high scientific relevance and also the most studied.[99, 103]

The biological media can contain thousands of biomolecules. The blood plasma alone has almost 3 700 identified proteins, thus allowing the formation of different combinations and organizations of coronas on nanoparticles.[97, 104] Despite the huge numbers of identified proteins, only a few dozens of proteins form the hard corona, since their affinity to the NP bare surface is very high, even if their current abundance in the biological fluid is low.[105-112]

According to Lundqvist's work, the proteins identified in the surface of nanoparticles incubated in human plasma can be organized in six main groups: immunoglobulins, apolipoproteins, which are responsible for the transport of lipids and cholesterol in the bloodstream, proteins from the complement pathways, a very crucial system in the innate immunity, and acute-phase proteins, also part of the immune system and that share some of its proteins with the complement pathways. The last two groups include coagulation factors, like fibrinogen or factor V, and other proteins like clusterin, serum albumin and vitronectin.[92]

Such variety could indicate that each nanoparticle would have a unique biological identity. But, even though the composition of the different particle-protein organizations in biological media may vary, if well-designed dispersion protocols are used throughout the experiments, one will achieve a high level of reproducibility of the populations of different particle-protein organizations, allowing a rational and reproducible approach to the study of bionanoparticle interactions with living organisms.[99]

As previously mentioned, the interaction between a cell and a nanoparticle will be mediated through the "protein corona". For a given nanoparticle, only several dozen proteins bind in significant amounts and for long enough to be biologically significant and recognized by the cell.[97] The recognition can either be generic or highly specific,

involving receptor-ligand interactions and leading to the binding of the nanoparticle to the cell, mediated by the corona. Such event will lead to its internalization, with a previous possible reorganization of the cell's membrane.[113, 114]

The interaction between both sides will only be possible if the protein corona has a slower exchange with other proteins present in the medium, compared with the time it takes for the particle to attach to the cell surface. This way, the corona (very likely the "hard" corona) will affect and mediate the nanoparticle-cell interaction.[104] But it is also possible that the proteins are not recognized by any membrane receptor (these are called bystander proteins in such situations) or they may be bound to the particle without presenting any relevant receptor-binding sequence. Compared to these, bare nanoparticles have a greater non-specific affinity to the cell surface and consequent internalization.[104] As a consequence, the cellular uptake of the nanoparticle-protein complex depends also on the presence of membrane receptors for the proteins present in the corona, and as along as the proteins are presented in the correct orientation favoring the interaction with the receptor, and as along as the nanoparticle-bound protein can compete effectively with the free proteins for the receptor.[104]

Although the extremely relevant effect of the protein corona in nanoparticle cell uptake is already widely accepted very little is still known about the effects of the corona and the proteins involved mainly due to its complexity and influencing parameters.[115] The adsorption may also cause conformational changes in the proteins structure[116], changes in membrane activity, transport processes, aggregation, avidity, and cell signaling.[7, 87, 117] In a way, with new alterations happening at the protein corona, a new biomaterial will be presented to the cells based on the combined effects of the NPs' physicochemical properties and the altered biological functions of the adsorbed proteins.[116] Consequently, what will happen when a NP approaches a cell, if the proteins at the corona will have their conformations altered, if the membrane itself will be changed, or if any other phenomena may happen, are still essentially unanswered questions.[12]

With the corona itself being modulated by the physicochemical properties of the nanoparticles, the resulting combination will dictate the NPs' pharmacokinetics and pharmacodynamics, the cell's uptake efficiency, the internalization pathway selection, the intracellular location, and cytotoxicity. [22, 45, 66] But these parameters are not totally dependent on the nanoparticle and its corona, but are also dependent on cell-specific characteristics such as cell type or cell cycle phase.[118]

Cell-type specific variation in the processing of NPs can be expected, since even in closely related cell lines, significant differences in intracellular sorting, trafficking and localization of non-conjugated quantum dots (QDs) were reported (three lines of human prostate cancer cells).[119] Also, the polyvalent surface of NPs may induce cross-linking of cellular receptors, starting signaling processes, initiating structural alterations at the cell surface, and interfere with normal cell function.[85, 120] Another aspect to consider, when studying cellular uptake of nanoparticles, is that the rate of endocytosis may also depend on the cell density.[121, 122]

In order to contribute to answer some of these questions the present work is aimed at evaluating how nanoparticles size and the protein corona affect nanoparticle internalization in a broad range of cell lines. Different *sera* will be used, most likely giving rise to distinct protein coronas, which will in turn be influenced by the size of the nanoparticle. Understanding, and eventually manipulating, the interplay between nanoparticles characteristics, protein corona formed and the endocytosis mechanism for a specific target cell population (like tumor cells), may constitute a major step towards more efficient nanomedicines.

2. Aim

The purpose of this thesis is to study the role that adsorbed proteins in the cellular internalization of nanoparticles (NPs), as a function of NP size, type of serum used and cell type.

3. Materials and Methods

3.1. Materials

Red dye-loaded (excitation/emission wavelengths – 580/605 nm) fluorescent carboxyl-modified polystyrene NPs (Fluospheres® size kit, ThermoFisher®) were used without any modification or purification. Sizes used in this work were 20, 40, 100, 200 and 500 nm. All stock solutions were stored at 4ºC, and used within 1 year of purchase, in order to ensure their stability.

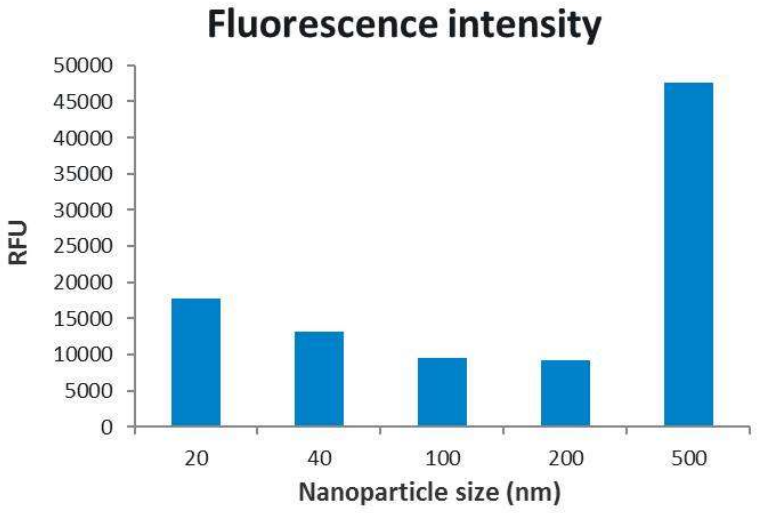

Figure 2 - Respective fluorescence intensity value of each different sized-nanoparticle. As it can be seen, the particles with nominal size of 500 nm possess the biggest fluorescence intensity, among the range of used NPs.

Human embryonic kidney Hek293t cells (passage 10-15), Human cervix epithelium Hela cells (passage 3-10), human stomach adenocarcinoma cells MKN28 (passage 30-50), human stomach adenocarcinoma cells MKN28 (CD44 variant domain 6 positive (CD44v6 +), passage 5-9), human gastric adenocarcinoma AGS cells (passage 2-9), human diffuse gastric carcinoma cells GP202 (passage 10-16) and a human bone marrow derived mesenchymal stem cells (hMSC, passage 2-9) were used. All cell lines were available from the i3S/INEB BioBank, except both MKN28 cell lines, which were supplied by Carla Oliveira (Expression Regulation in Cancer, i3S).

A broad range of cell lines was used to understand how the NPs internalization plays out on several tissues and organs. With the exception of Hek293t and hMSC, most of these are cancer cell lines, stomach derived, due to the work and interest the

group has in this area.[123, 124] Furthermore, two similar cell lines, MKN28 expressing or not CD44v6 were also used. CD44 is a known cell-surface glycoprotein involved in cell-cell interactions, cell adhesion, and migration.[125] Certain CD44 variant isoforms, especially those containing CD44v6 have been implicated in oncogenesis, tumor cell invasion and metastasis, primarily associated with epithelial derived tumors. In nonmalignant tissues, CD44v6 expression is essentially restricted to a subset of epithelia.[126-129] Being two similar cell lines, their use here was destined to check if the presence/absence of CD44v6 altered the NP uptake of the cell. Since CD44 is a glycoprotein involved in cellular interaction and adhesion, the possibility of it having significant changes in the NP uptake between the two cell lines was presumed, although this possibility was expectedly low.

Two cell culture media were used in this work: Roswell Park Memorial Institute Medium 1640, with [+]-L-glutamine (RPMI, Gibco©), and Dulbecco's Modified Eagle's Medium (DMEM, Gibco©).

Different types of serum were used to allow the study of the influence of the protein corona formed on NPs, namely: fetal bovine serum (FBS, Biowest), "proprietary blood fraction" (PBF, Orthosera, Austria) and human albumin (HA, Biotest). Complete medium (CM) was the designation used to refer to medium supplemented with serum, while serum free medium (SFM) was medium without any serum, equivalent to a 'no serum' condition.

The PBF serum, produced by Orthosera, is a specific, growth-factor rich human serum fraction, which has shown superior effects in promoting cell proliferation in osteoarthritic bone and cartilage cells.[130] As part of a collaboration, we are studying the potential of this serum, on behalf of Orthosera. All samples of PBF were obtained from the same donor.

FBS serum was chosen, since it's also a rich type of serum. This way comparison between the results obtained in this condition, with the 'PBF' condition, is possible. While HA serum was chosen, since it was the simplest type of serum, containing only human albumin. It's known that albumin is also present on FBS and PBF serums.

3.2. Cell Culture

MKN28 (CD44v6 -), AGS, GP202, HeLa, Hek293t cells were cultured at 37ºC in 5% CO_2 in RPMI Medium 1640 (Gibco©) supplemented with 10% fetal bovine serum (FBS, Biowest) and 1% penicillin/streptomycin (Biowest).

hMSC cells were cultured at 37ºC in 5% CO_2 in Dulbecco's Modified Eagle's Medium (Gibco©) supplemented with 10% FBS (HyClone, GE Healthcare Life Sciences©) and 1% penicillin/streptomycin. A different FBS was chosen, since there are certain differences between two FBS produced by different companies, and the hMSC cells grow faster in cDMEM, supplemented by FBS (HyClone).

MKN28 (CD44v6 +) cells were cultured at 37ºC in 5% CO_2 in RPMI Medium 1640 (Gibco®) supplemented with 10% foetal bovine serum (FBS, Biowest) and 1% Geneticin® (G418) Sulfate (ThermoFisher©).

All cell lines were confirmed to be mycoplasma negative through PCR analysis involving specifically designed primers to detect mycoplasma DNA. These tests were done monthly.

3.3. Determination of Serum Protein Content

Different serum percentages were used to ensure the same protein content in that each condition. To determine the protein content, the colorimetric BCA Protein Assay kit (ThermoFisher®) was used. The measurements were performed on a SynergyMx, BioTek®. The absorbance was read at 655 nm.

After determining the protein content of each serum, the % equivalent of PBF and HA in CM was calculated in order to achieve the same protein content as 10% FBS, which corresponds to the usual % of serum added to cell culture medium to obtain CM. The following table contains the percentage of serum volumes that were required to ensure that, in the end, the same protein content was present is all conditions tested.

Table 2 – Serum % range used in complete medium (CM) throughout the work whenever new aliquots were prepared and assayed with BCA Protein Assay kit.

Serum	Serum % added to SFM
FBS	10 %
PBF	10.7 – 11.4 %
HA	16.4 – 20.5 %

Whenever a new aliquot of serum was needed, a new BCA protein assay was performed on all the *sera* used to ensure that all work conditions had the same protein content.

3.4. Formation of Protein Corona on NPs

NP dispersions were prepared by diluting the concentrated stock solutions in complete medium (DMEM or RPMI; supplemented with the different % of *sera* defined in item 2.3) or serum free medium (SFM) used for cell culture at room temperature, immediately prior to the experiments on cells, with an identical time delay between diluting and introducing NPs to the cells for all experiments. Before sampling, NPs were vigorously mixed by vortexing for 30s. After the addition of the NPs to the different incubation solutions, these were also vortexed for 15s to ensure maximum NPs dispersion.

3.5. Characterization of Nanoparticles

The mean size and surface charge of NPs were determined using a photon correlation spectrophotometer (Malvern Zetasizer Nano ZS). The mean size is related to the hydrodynamic diameter, measured through the Dynamic Light Scattering (DLS) technique, and surface charge is related with zeta potential, determined through laser Doppler Micro-eletrophoresis (DME). Measurements were performed at 25ºC in phosphate-buffered saline (PBS) solution and in RPMI, without serum or supplemented with the different *sera* with the appropriate %, to ensure same protein content, as determined in item 3.3.

3.6. NPs Uptake by Cells

$40x10^3$ or $20x10^3$ (uniquely for hMSC) cells were seeded in 24-well plate (Falcon®) and incubated for 48h prior to the addition of NPs. Afterwards, cells were incubated with culture medium supplemented with the different *sera* under study and the differently-sized NPs for 24h. The final concentration of NPs used in the incubation solution was 20 μg/mL, a concentration used in past uptake experiments and one that didn’t present any signs of toxicity. Negative controls consisted in the several serum

conditions but without NPs. For time profiles experiments the incubation time was of 30 min, 1, 3, 6 and 24h.

After this incubation time, the medium was removed and the samples were washed thrice with PBS (1x), to ensure particle removal from the outer cell membrane. The fluorescence intensity of all PBS washes of the 24-well plates demonstrated the efficiency of the washes, following particle removal. Cells were then trypsinized for 5 min at 37ºC. After cell detachment confirmation, CM was added to neutralize the trypsin and all the content transferred to polystyrene round-bottomed tubes (Falcon®), before samples were immediately analyzed by flow cytometry.

3.7. Analysis of NPs internalization by Flow Cytometry

NPs internalization was analyzed immediately after their incubation with cells using a fluorescent-activated cell sorter (FACS) Calibur (BD Biosciences©) flow cytometer. The results are reported as the mean of the distribution of cell fluorescence intensity obtained by measuring 2000-10 000 cells (depending on each cell line), averaged between 2 independent replicas of 3 independent experiments. Error bars correspond to the standard deviation between these 3 independent experiments.

For the imaging cytometry analysis, the same protocol described previously for sample preparation of the flow cytometry, was used. Samples were analyzed on an imaging flow cytometer ImageStreamX© (Amnis, EDM Millipore), acquiring at most 10 000 cells at the Bioimaging Center for Biomaterials and Regenerative Therapies (b.IMAGE, i3S). A 488 nm wavelength laser was used to excite NPs fluorescence, which was collected using the 595–660 nm spectral detection channel (Ch04). Other instruments setting included the following: 488 nm laser power: 10.00; 785 nm laser power: 11.00; Cell Classifier: area upper limit Ch01 – 400, area lower limit Ch01 - 40. The analysis of multiple image-based parameters was performed using the IDEAS software (v6.2.64, Amnis Corporation, EDM Millipore). The Internalization feature was used to evaluate the obtained results.

4. Results and Discussion

4.1. Protein Quantification in Different Types of Serum

In order to ensure that each condition (media supplemented with FBS, PBF or HA) had the same protein content, avoiding the excess/deficit, in terms of protein content, that could influence the results, the BCA protein quantification assay kit was used to determine total protein concentration in each serum type used. This kit was chosen due to its simple protocol, high linearity and fast reaction time. The kit is provided with standard albumin samples to be assayed and used to produce a calibration curve. The example provided in Table S2 and S3 demonstrates how it was used to determine the protein content.

Using the equation from the calibration curve (Fig. S1), it was possible to determine the protein content in each serum type under study and thus determine the volume of each serum required and used in serum free medium (SFM) to keep the protein content constant in every condition tested.

4.2. Influence of Serum Type on Protein Corona Formed

Carboxylated-modified polystyrene NPs with nominal sizes of 20, 40, 100, 200, and 500 nm were selected as the model particles in order to understand the influence of size, combined with different protein corona, in their internalization by different cell lines. These NPs were chosen since they are widely available to the scientific community, have been extensively studied, present low toxicity and have already been used by the group in past uptake experiments.[131-133] A large range of sizes was used to allow a more in depth characterization.

The NPs characterization was done, using a zetasizer, to evaluate particle size, polydispersity, charge and relative permittivity of the different particle dispersions produced in this work.

Table 3 - Polystyrene NPs characterization after incubation in PBS buffer or in cell culture medium supplemented with the different *sera* in study (FBS, PBF and HA), or without serum (no serum). Results here are presented as mean ± S.D., averaged from three independent measurements, of one independent experiment.

NP initial size (nm)	Medium supplementation	Size (nm)	PDI	Charge (mv)	ε (μm.cm/v.s)
20	PBS	34.36 ± 0.67	0.217 ± 0.009	-31.93 ± 1.03	16.3 ± 0.4
	No Serum	60.68 ± 1.60	0.286 ± 0.040	-24.43 ± 1.51	15.1 ± 0.4
	FBS	72.69 ± 9.81	0.462 ± 0.219	-8.09 ± 0.81	15.8 ± 1.3
	PBF	59.57 ± 3.22	0.822 ± 0.034	-7.54 ± 0.83	14.3 ± 0.4
	HA	19.23 ± 0.86	0.757 ± 0.022	-8.17 ± 0.60	13.5 ± 1.0
40	PBS	50.78 ± 0.38	0.039 ± 0.016	-35.40 ± 1.18	17.0 ± 0.6
	No Serum	53.81 ± 0.71	0.035 ± 0.016	-21.86 ± 1.03	14.9 ± 0.7
	FBS	53.25 ± 0.29	0.514 ± 0.001	-9.71 ± 0.09	14.7 ± 0.5
	PBF	63.18 ± 2.50	0.833 ± 0.038	-9.55 ± 1.04	14.3 ± 0.4
	HA	44.94 ± 7.91	0.478 ± 0.080	-10.01 ± 0.60	12.7 ± 0.3
100	PBS	109.27 ± 1.25	0.012 ± 0.011	-39.07 ± 1.37	16.8 ± 0.5
	No Serum	117.20 ± 7.62	0.107 ± 0.003	-23.50 ± 1.39	15.2 ± 0.6
	FBS	160.07 ± 5.26	0.285 ± 0.001	-9.27 ± 0.49	15.2 ± 1.0
	PBF	104.85 ± 10.52	0.482 ± 0.051	-7.30 ± 0.17	16.1 ± 1.0
	HA	104.76 ± 31.40	1.000 ± 0.000	-7.95 ± 0.56	14.0 ± 1.0
200	PBS	215.27 ± 1.75	0.012 ± 0.009	-35.23 ± 2.66	17.2 ± 0.5
	No Serum	210.83 ± 6.07	0.021 ± 0.021	-26.57 ± 1.29	15.0 ± 0.6
	FBS	288.90 ± 17.13	0.235 ± 0.011	-9.81 ± 0.39	15.2 ± 0.9
	PBF	185.73 ± 5.08	0.535 ± 0.037	-7.41 ± 0.15	15.1 ± 0.6
	HA	182.60 ± 9.00	0.606 ± 0.024	-9.34 ± 0.79	13.4 ± 0.5
500	PBS	568.87 ± 4.90	0.103 ± 0.015	-33.83 ± 1.59	16.6 ± 0.5
	No Serum	556.33 ± 25.72	0.267 ± 0.044	-22.57 ± 3.10	15.1 ± 0.6
	FBS	614.20 ± 110.16	0.629 ± 0.088	-8.92 ± 053	15.4 ± 0.8
	PBF	710.07 ± 39.22	0.659 ± 0.047	- 7.45 ± 0.15	15.3 ± 0.6
	HA	670.83 ± 43.32	0.615 ± 0.135	-10.72 ± 1.12	13.4 ± 0.8

As can be depicted from Table 3, NPs showed similar sizes to their nominal sizes and high levels of monodispersity (PDI < 0.3), when measured in PBS buffer, as it would be expected, indicating there's a low heterogeneity of particle sizes in the solution.[134] The differences between the nominal size and the measured size are mainly due to the DLS technique not being very sensitive to such small particles.[38]

Some levels of aggregation were to be expected when NPs were dispersed in medium supplemented with different *sera*, since in those conditions NPs have a tendency to aggregate, leading to an increase in size and to PDI values > 0.3, indicating a higher heterogeneity of particle sizes dispersed.[134] This was also due to the fact that the DLS technique used quantifies size distributions and its results are

influenced by NPs aggregation.[38] This was verified in most NPs dispersed in medium supplemented with different *sera*, where the hydrodynamic diameter was superior to the nominal size, and was especially true in all NPs sizes dispersed in medium supplemented with FBS and in all 500 nm NPs dispersed in the medium supplemented with different *sera* (Table 3).

A few exceptions was also observed, namely 20 nm NPs dispersed in CM, supplemented in HA, presented an hydrodynamic diameter very close to 20 nm, but with a PDI value of 0.757.[134] And 200 nm NPs dispersed in medium supplemented with PBF and HA, also had a smaller hydrodynamic radius than expected, combined with a PDI value bigger than 03. Perhaps this can be due to the presence of lower levels of serum protein aggregates, which will influence the size measurements.

It is worth mentioning that, according to literature, the formation of a protein corona does not usually alter the hydrodynamic diameter significantly, when comparing it to a bare nanoparticle (without a protein corona). The thickness of the protein corona is usually around 4 to 10 nm. Hence, the more significant differences of hydrodynamic diameter observed are probably due to aggregation and the formation of several NP-protein multimers.[99] For instance, Nienhaus *et al*. determined the thickness of a monolayer of human serum albumin on 10-20 nm polymer coated FePt and CdSe/ZnS nanoparticles to be of 3.3 nm, indicating that the hydrodynamic diameter changes probably are most likely a results of the formation of multimers and not solely due to the presence of protein corona.[135]

Zeta potential measurements indicated the superficial charge of NPs and were also used to indicate the stability behavior of a colloid dispersion: the more positive it was, the more stable the colloid dispersion was. Zeta potential measurements (Table 3) showed that NPs were negatively charged, after incubation in PBS buffer or medium without serum, which was expected since they are carboxylate modified. They had similar values since all used NPs, regardless of size, have the same composition and modification. The surface charge of the particles dispersed in PBS were more negative (approximately -35 mV) than the particles dispersed in SFM (approximately -23 mV). This was probably due to the presence L-glutamine in the SFM (the RPMI medium), with amine positive groups, which helped stabilize the NPs more than the cations present in PBS buffer. The lower negative charges in serum supplemented with the different *sera* can be explained by the protein adsorption on the NPs surface (Table 3). Dawson *et al*. suggested that this is due to a different dispersion stabilization mechanism (involving charge and steric hindrance) from the typical one for bare NPs.

This stabilization is likely conferred by specific protein layer characteristics, where the entire protein complex surrounding the NP is colloidal stable, despite the crowded environment.[99]

The dielectric constant (ε, also called relative permittivity) measurements served as controls and were approximately 15 μm.cm/V.s for the NPs dispersed in SFM and in medium supplemented with the different *sera*, and 16 μm.cm/V.s in PBS (Table 3). The minor differences found in these measurements, namely between the medium supplemented with different *sera*, were probably due to each serum having a distinct composition, which altered the dielectric constant of the solution.

4.3. Assessment of NPs Internalization by Flow Cytometry

Flow cytometry was used to measure average cell fluorescence intensity after incubation with 20 μg/mL of fluorescently labeled NPs for 24h. Since each nanoparticle size used has a respective mean fluorescence intensity, results will be presented in terms of fold increase (fluorescence intensity of cell incubated with NPs/untreated cells), comparing only between serum conditions. Furthermore, in order to verify that all fluorescence measurements were due to nanoparticles internalized in the respective cells, the efficiency of the washes was verified and the results are shown in Figs. 3 and S1, for GP202 and MKN28 (CD44v6 -) cell lines.

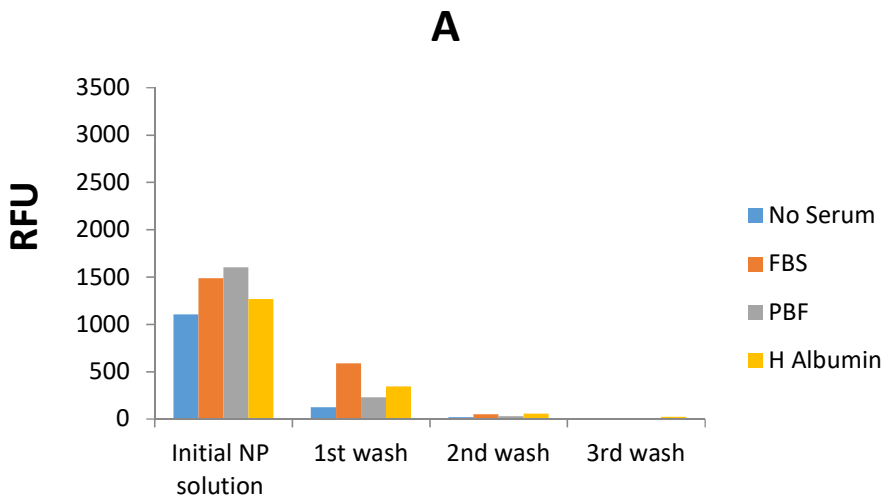

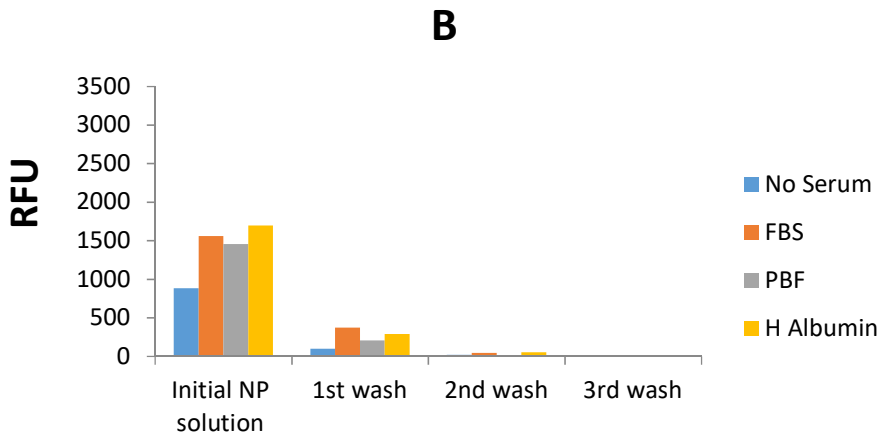

Figure 3 - Fluorescence intensity results of the 40 NP solution used to incubate cells and supplemented with different *sera*, before incubation and after three washes. (A) MKN28 (CD44v6c -) cells, (B) GP202 cells.

The efficacy of the three washes was thus demonstrated since the fluorescence intensity values remaining in the third wash were very low, comparing to the intensity levels of the initial NP solution.

Afterwards, the influence of NP size and the respective protein corona (after pre-incubation in the different *sera*) on the NPs uptake (during 24h), across various cell lines, were studied and results are shown in Fig. 4. Our main interest here was to compare the results obtained in the 'no serum' condition with the 'PBF' condition. Since PBF serum is a human rich type serum, currently being used by Orthosera in their medical experiments, and prepared from blood samples of the same donor. While FBS is pooled from different animal donors and there wasn't an interest in applying a statistical treatment to these results, due to the possible inconsistences between FBS batches. And, in the 'HA' it simply served as control, since it was a very simple serum.

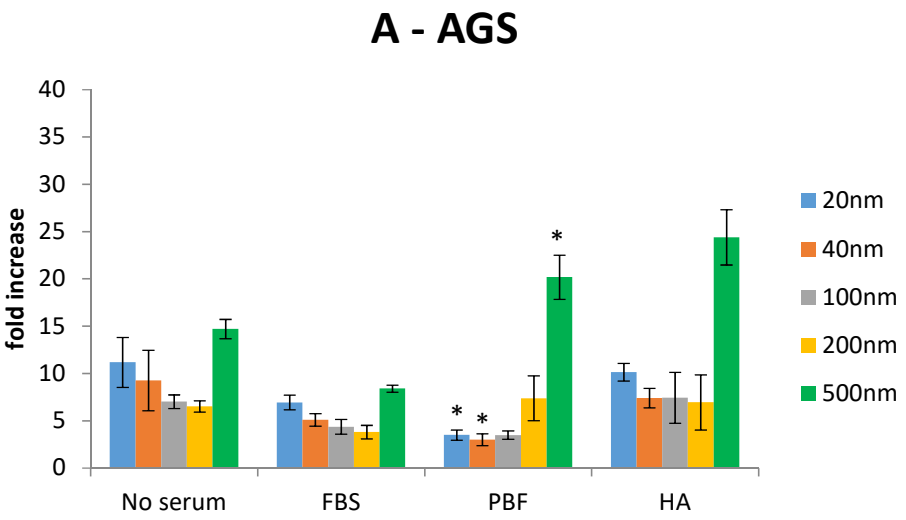

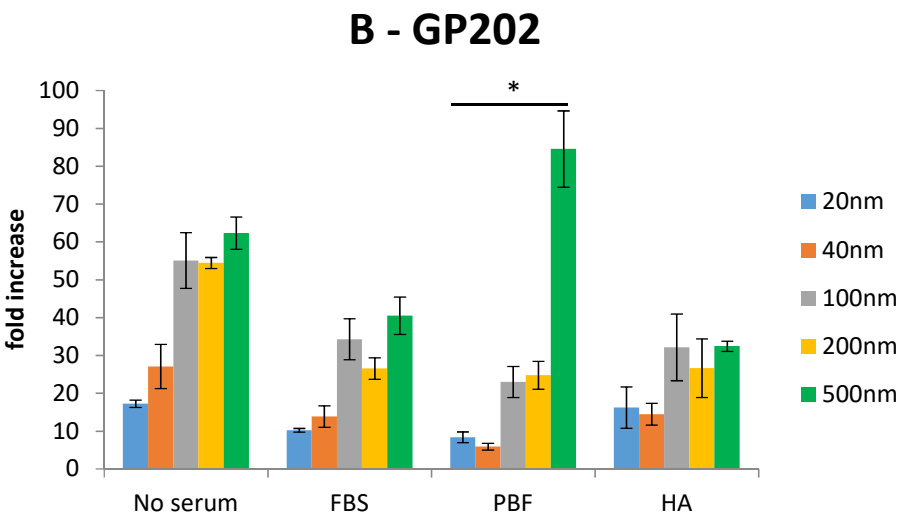
B - GP202
fold increase
100
90
80
70
60
50
40
30
20
10
0
*
No serum
FBS
PBF
HA
20nm
40nm
100nm
200nm
500nm

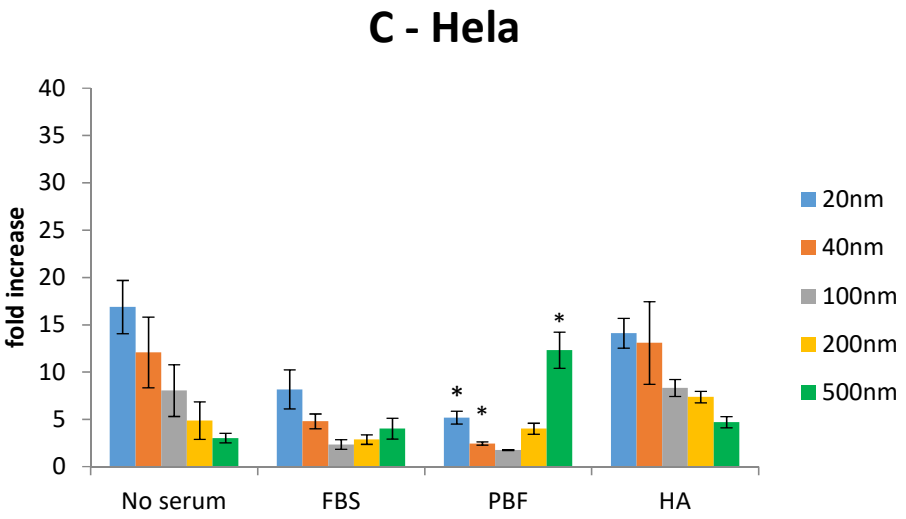
C - Hela
fold increase
40
35
30
25
20
15
10
5
0
*
*
*
No serum
FBS
PBF
HA
20nm
40nm
100nm
200nm
500nm

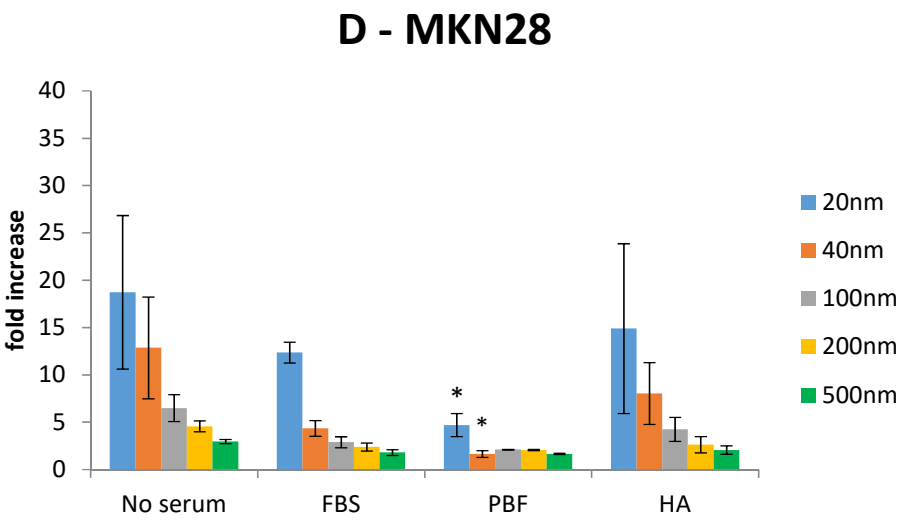
D - MKN28
fold increase
40
35
30
25
20
15
10
5
0
*
*
No serum
FBS
PBF
HA
20nm
40nm
100nm
200nm
500nm

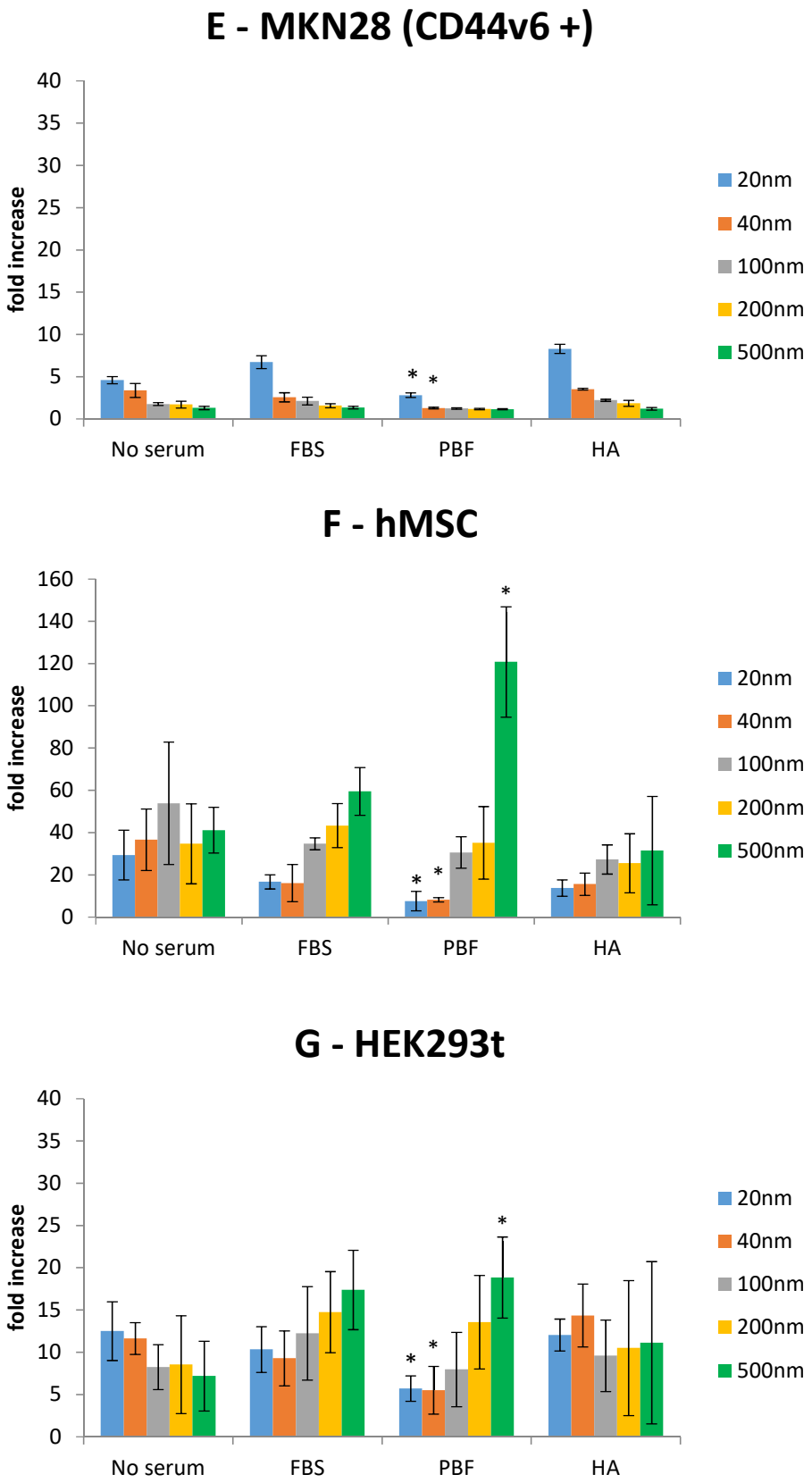

Figure 4 - Influence of NP size and protein corona on the NPs uptake (during 24h) across various cell lines. (A) AGS cell line; (B) GP202 cell line; (C) HeLa cell line; (D) MKN28 cell line (CD44v6 -); (E) MKN28 cell line (CD44v6 +); (F) hMSC cell line; (G) HEK293t cell line. Results are reported as fold increase ± S.D. of NPs uptake relative to cells that were not

exposed to NPs, averaged between two replicas of three independent experiments. * t < 0.05, compared with respective NPs size in the No Serum condition.

In terms of the influence of the different protein corona and NP size on cell uptake, results show a clearly distinct behavior especially when observing 20, 40 and 500 nm NPs. For the 20 and 40 nm NPs, results show that protein adsorption on their surface decreased their subsequent uptake by the different cells quite significantly, clearly observed when comparing conditions without serum and/or 'FBS' and 'PBF', as was reported in other works concerning the uptake of polystyrene nanoparticles.[134, 136] In fact, when nanoparticles were exposed in the absence of serum in the culture medium, significantly higher uptake was obtained. The reason behind this phenomenon was probably due to hydrophobic effects. When bare polystyrene nanoparticles were administrated to cells, their high surface hydrophobicity may cause them to adhere to the already hydrophobic plasma membrane.[137] On the other hand, in the presence of serum, adsorption of proteins probably diminished the non-specific hydrophobic binding of the nanoparticles to the cell surface, leading to a decrease of the surface hydrophobicity and a consequently lower, but more specific, uptake of the nanoparticles via cellular receptors.[137, 138]

Surprisingly, opposite results were obtained when nanoparticles with 500 nm were used, where a clear inversion of behavior can be observed, especially when comparing 'no serum' and 'PBF' conditions. This phenomenon could be explained by the existence of a particular group of proteins (in a certain ratio) in the protein corona composition of these 500 nm NPs that were able to activate the cellular machinery in a different manner in this NP size, increasing their respective internalization. Other possible explanation could involve the conformation and orientation of the adsorbed proteins in the corona that may expose different and/or more recognizable domains which leads to a bigger NPs uptake.

Results for MKN28 cell lines (Figs. 4D and E), expressing or not CD44v6, showed that the difference of uptake between "no serum" and "PBF" for 500m, verified previously, didn't occur in this case; an increase in the uptake of 500 nm particles was not observed, when compared with the "no serum" condition. More experiments are required to explain this difference of behavior, although we hypothesized that it may be due to differences of proteomic profile between all the cell lines studied. Nevertheless, between MKN28 and MKN28 (CD44v6 +), they showed similar internalization profiles, although the latter has a slightly smaller fold increase across all conditions and NPs sizes. This could be due to the fact that MKN28 cells, expressing CD44v6, having an

increased cell-cell adhesion, which may be responsible for compromising the internalization of NPs. The presence/absence of CD44v6, didn't impact the internalization of NPs, as it was expected.

Also, the uptake of 500 nm NPs exhibiting a protein corona originated from FBS and HA, both seemed higher than the uptake of bare 500 nm NPs ('no serum' condition), like in the case of the HeLa or Hek293t (Figs. 4C and G, respectively), or lower, as in the case of GP202 (Fig. 4B). But, as it can be seen, AGS and hMSC do not follow this pattern (Figs. 4A and F).

Overall, it seems that smaller NPs (20-200 nm), with a protein corona formed with PBF proteins, result in a lower uptake when compared to equally-sized NPs present in SFM. But, as the NPs become larger and reach 500 nm, after coating with proteins derived from PBF, their uptake was higher than their equivalents in the no serum condition, except for both MKN28 cell lines.

In terms of fold increase, hMSC had the highest uptake of 20 and 40 nm particles, in SFM or CM supplemented with FBS, while in the PBF and HA conditions, the uptake was essentially even across cell lines (Figs. 5A and B). But for NP sizes larger than 40 nm, it can be noticed that the two cell lines that resulted in the highest uptake, across all conditions, were GP202 and hMSC. Also in Figs. 5 C, D and E, the tendency mentioned before can be clearly observed between the 'no serum' and 'PBF' conditions, across all cell lines.

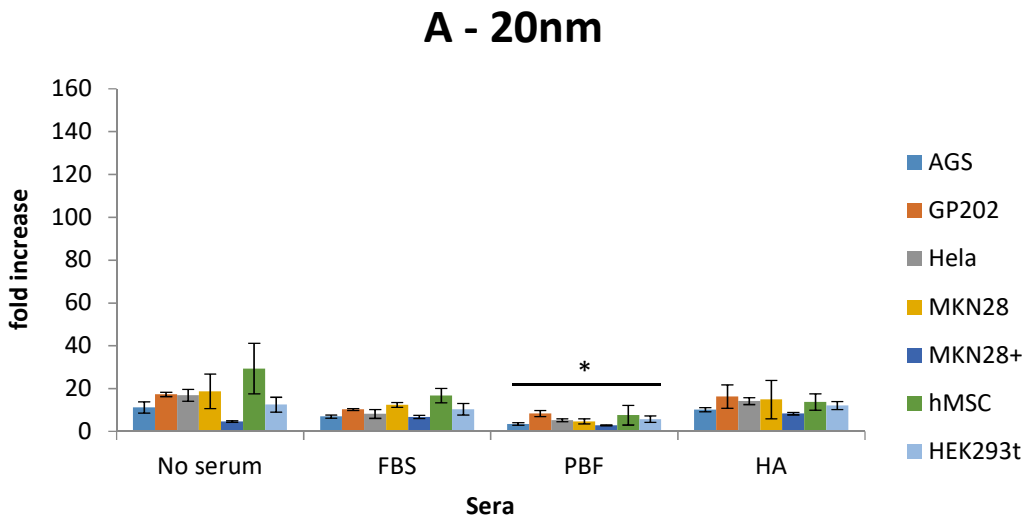

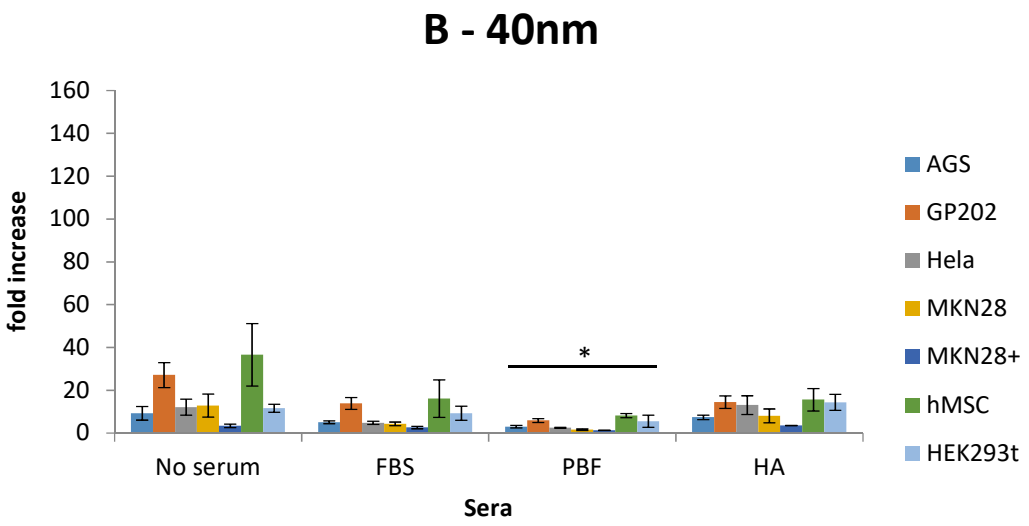
B - 40nm
fold increase
160
140
120
100
80
60
40
20
0
*
No serum
FBS
PBF
HA
Sera
AGS
GP202
Hela
MKN28
MKN28+
hMSC
HEK293t

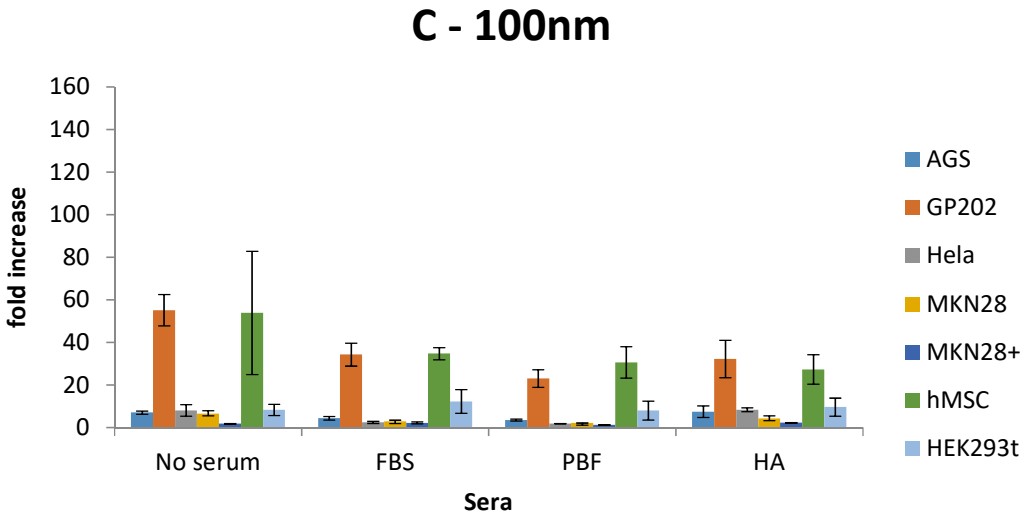
C - 100nm
fold increase
160
140
120
100
80
60
40
20
0
No serum
FBS
PBF
HA
Sera
AGS
GP202
Hela
MKN28
MKN28+
hMSC
HEK293t

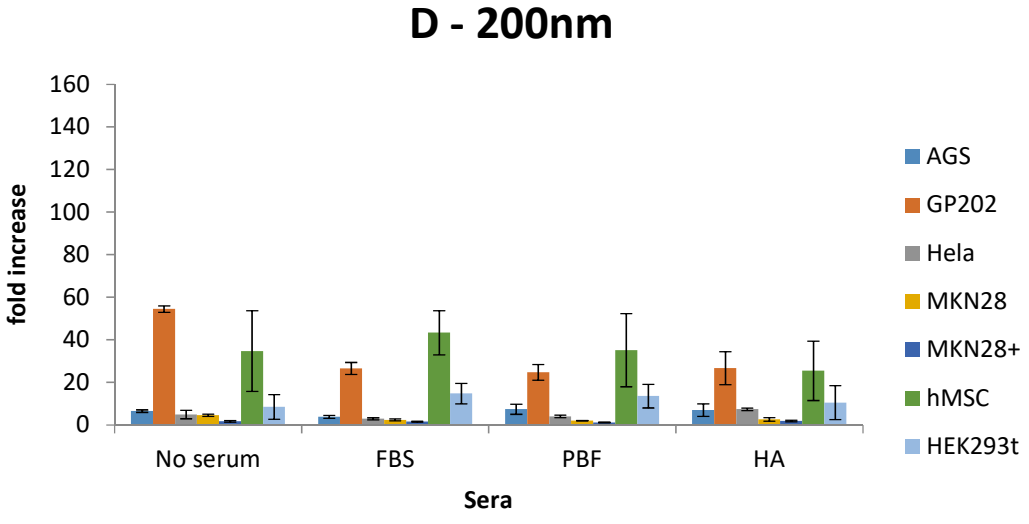
D - 200nm
fold increase
160
140
120
100
80
60
40
20
0
No serum
FBS
PBF
HA
Sera
AGS
GP202
Hela
MKN28
MKN28+
hMSC
HEK293t

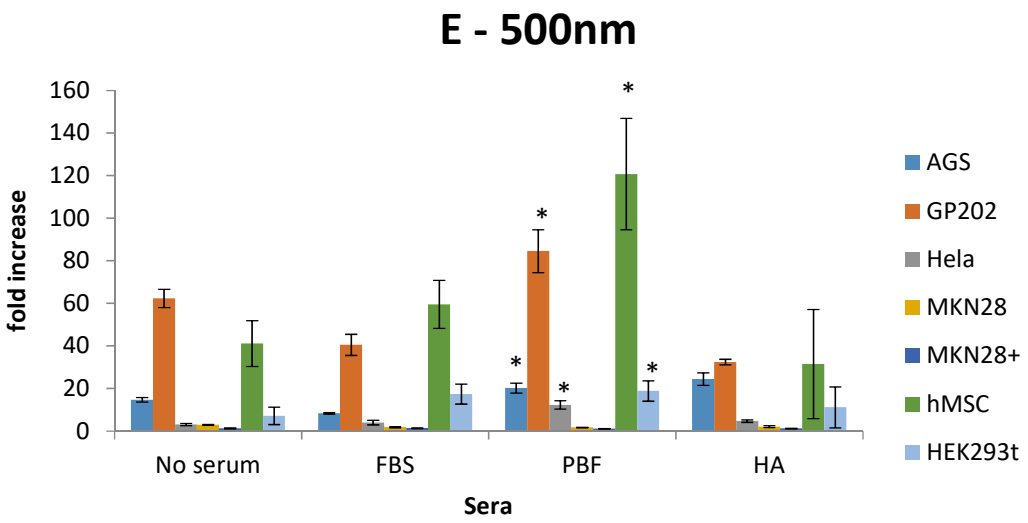

Figure 5 - Influence of protein corona and cell-type specificity on the NPs uptake (during 24h) in terms of NP sizer across different cell lines. (A) 20 nm; (B) 40 nm; (C); 100 nm (D) 200 nm; (E) 500 nm. Results are reported as fold increase ± S.D. of NPs uptake relative to cells that were not exposed to NPs, averaged between two replicas of three independent experiments. * $t < 0.05$, compared with respective cell line for each No Serum condition.

In general, when comparing NPs uptake by cancer cell lines and nonmalignant cell lines (like Hek293t and hMSC), no distinct pattern could be observed. A possible explanation for the higher uptake of NPs in hMSC and GP202 cell line might be due to an increased gene expression, but no literature was found concerning the matter at hand.

Some research works were published, studying protein corona formation as the result of blood fraction exposure and how it plays a major part in the internalization of resulting NPs.[136, 139-141] For example, Schöttler *et al*. reported distinct and major differences in the uptake of polystyrene NPs incubated in FBS, human serum, human citrate and heparin plasma. They found that heparin potentiated the uptake into macrophages, but they prevented internalization into HeLa cells, while human citrate seemed to had the most important results in the *in vitro* studies of NPs uptake.[136]

They also concluded the need to investigate the protein sources of the serums or plasma used to incubate the NPs, and to determine the composition of the hard protein corona, since there was a prominent difference not only between the human and bovine media, but also between serum and plasma (serum is depleted from coagulation factors, while plasma contains proteins from the coagulation system), and the anticoagulants used in the plasma generation.[92, 136, 142] Although PBF production is anticoagulant-free, the composition of each serum should indeed be determined, in order to compare the obtained results to other works.

The kinetics of NPs uptake was also studied using the GP202 cell line (Fig. 6). The same conditions were kept and only the NPs with nominal sizes of 40 and 500 nm were used in these experiments. These two sizes were chosen since they were proven to be statistically relevant for all cell lines (except MKN28 cell lines), when comparing the fold increase changes, in the SFM and in the medium supplemented with PBF.

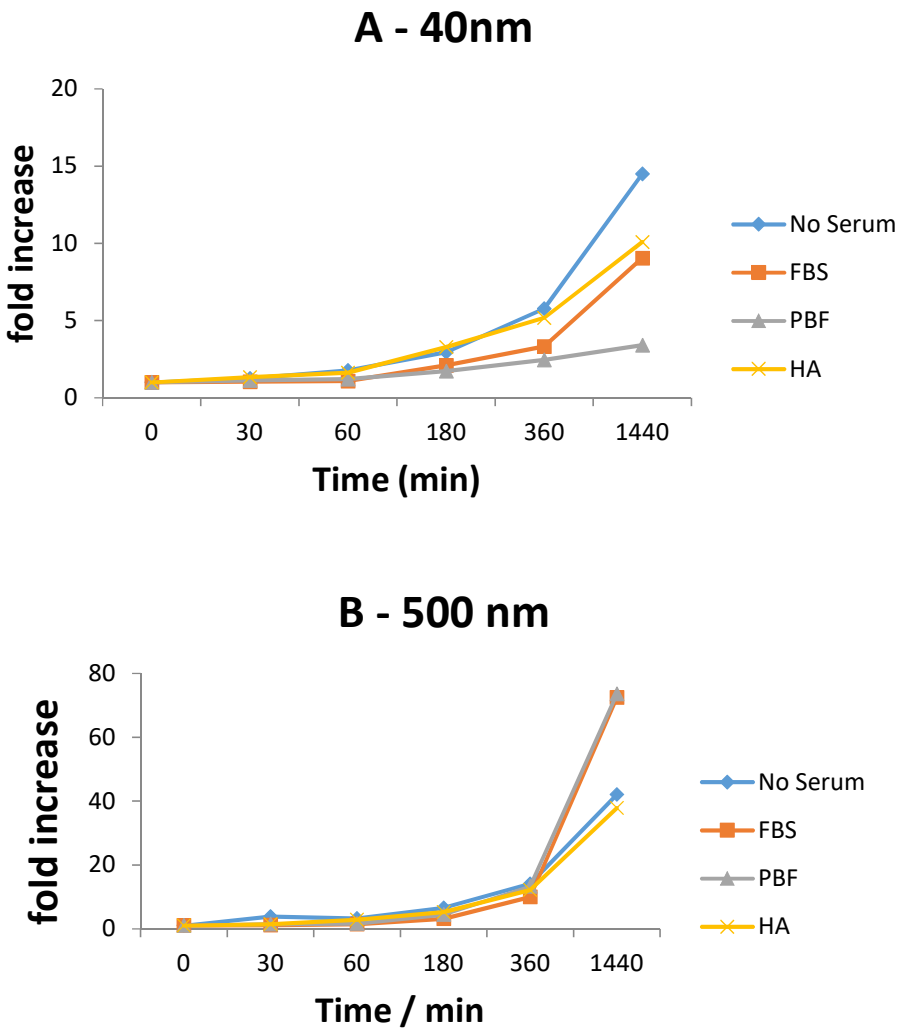

Figure 6 - Time profile of 40 and 500 nm NPs uptake in GP202 cell line. The same conditions were used and the time points chosen for this experience were 30 min, 1, 3, 6 and 24h. Results are presented as fold increase levels of NPs uptake, with respect to control cells that were not exposed to NPs, averaged between 2 independent replicas of 1 independent experiment.

In Fig. 6A, for the first 60 min, the fold increase remained very low and stable (fold increase level of approximately 1.5). But, after the 60 min, the NPs uptake steadily increased until the 1440 min time point (24h). Even though the results presented in Fig. 6 are from one single experiment, the fold increase levels at 24h demonstrate the same tendency of the results obtained in the previous experiments (Fig. 4B), with the same incubation period of 24h. The highest NPs uptake was observed using bare particles

(this value is lower than the correspondent one in Fig. 4B, which had a fold increase of 27.08). The rest of the fold increase levels were similar to the ones obtained in Fig. 4B, when comparing the results of NPs of the same size, incubated in the same medium conditions.

In Fig. 6B, for the first 60 min, the fold increased also remained stable and low, at an approximate level of 3. Then, after the 180 min time point, the fold increase in NPs uptake continued to grow bigger, among the different *sera* conditions. At 24h, the highest uptake happened with the 500 nm NPs with a PBF and FBS-originated protein corona, which had similar levels between them. This is different from our previous results, in Fig. 4B, where 500 nm NPs with a PBF-originated 'corona' were significantly more uptaken than the same-sized NPs with an FBS-originated 'corona'. The uptake of 500 nm particles in medium supplemented with HA was also similar to the uptake of same-sized NPs in SFM.

Also in Fig. 6B, the uptake of 500 nm particles, incubated in SFM, presented a small peak at the 30 min time point, but since these fold increase levels were only averaged between two independent replicas of one independent experiment, this could be meaningless, since it will be necessary to repeat this experience, at least two more times. It will also be interesting to see if the other cell lines used in this work will present a similar uptake pattern and if they demonstrate the same tendency that was reported in the flow cytometry results.

Cellular internalization was further characterized, for the first time, by Imaging flow cytometry, a recent technology that allows the fast imaging of a high quantity of cells in flow. It combines the speed and sensitivity for fluorescence intensity quantification of conventional flow cytometry with the morphological features discrimination of microscopy, for the specific location and distribution of signals within individual cells and in the whole cellular population.

For these preliminary experiments, cell uptake studies were only performed with NPs with the nominal sizes of 40 and 500 nm, under the same serum conditions as before, and using the Hek293t, HeLa, GP202, MKN28 (CD44v6 -) and AGS cell lines. The internalization feature of the IDEAS software was used to obtain the results seen in Fig. 7, while more detailed information can be found on Table S4 and Fig. S3, the latter describing the process of using the internalization feature. Internalization score is defined as the ratio of the intensity inside the cell to the intensity of the entire cell. The higher the score, the greater the number of NP inside the cell. Therefore, it was important to define the inside (cytoplasm) and the membrane of the cell for this

measurement. For the calculus of the median value of the internalization score, only cells with an internalization score > 0 were considered (defined in Fig. S3D as Internalization positive). Cells with a negative internalization score have a greater NP intensity at the cellular membrane level, than compared with the intensity inside the cell, therefore they were excluded from the calculations.

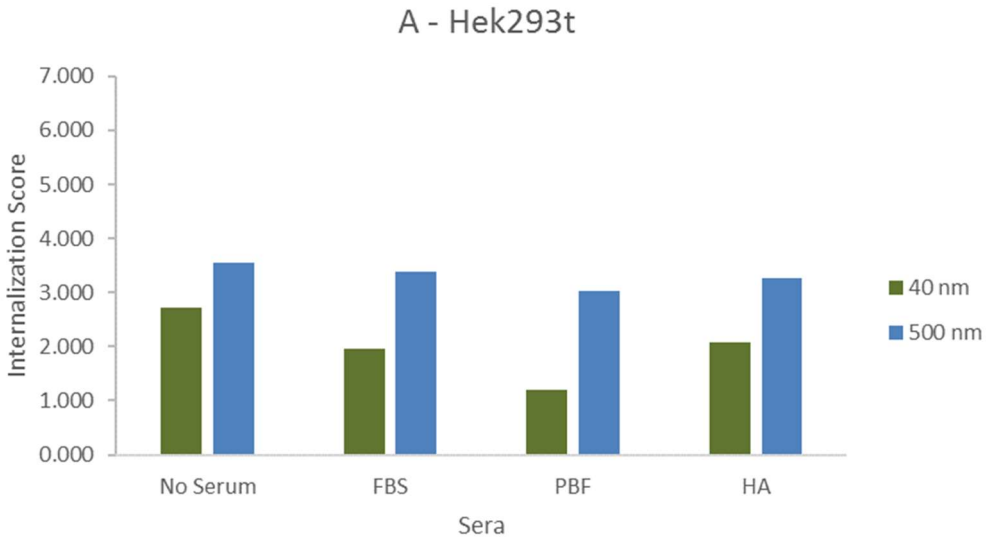

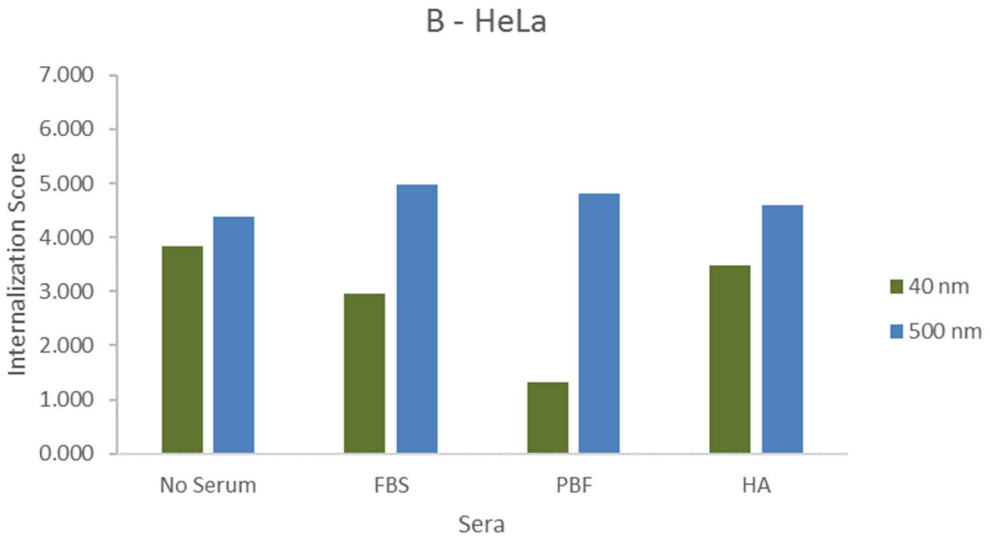

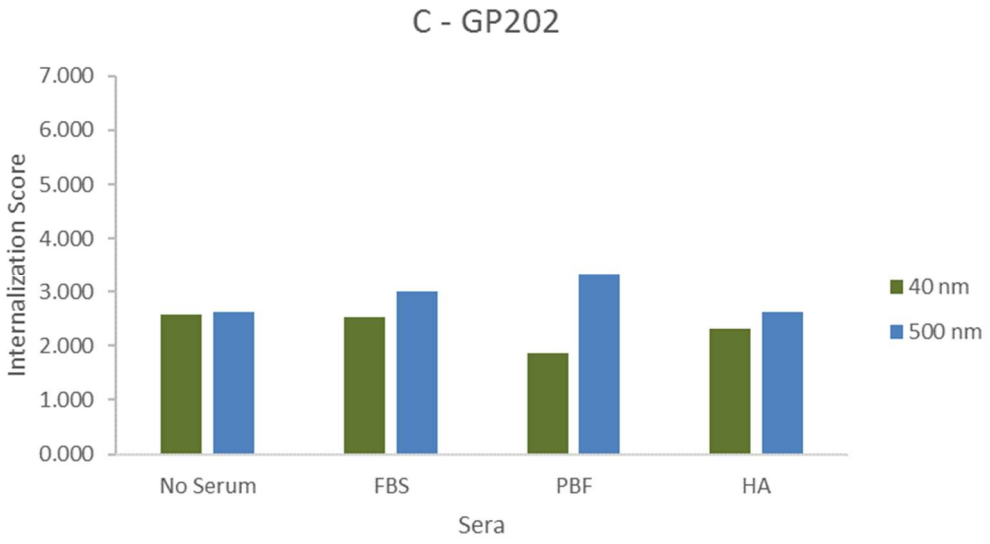
C - GP202
Internalization Score
7.000
6.000
5.000
4.000
3.000
2.000
1.000
0.000
No Serum
FBS
PBF
HA
Sera
40 nm
500 nm

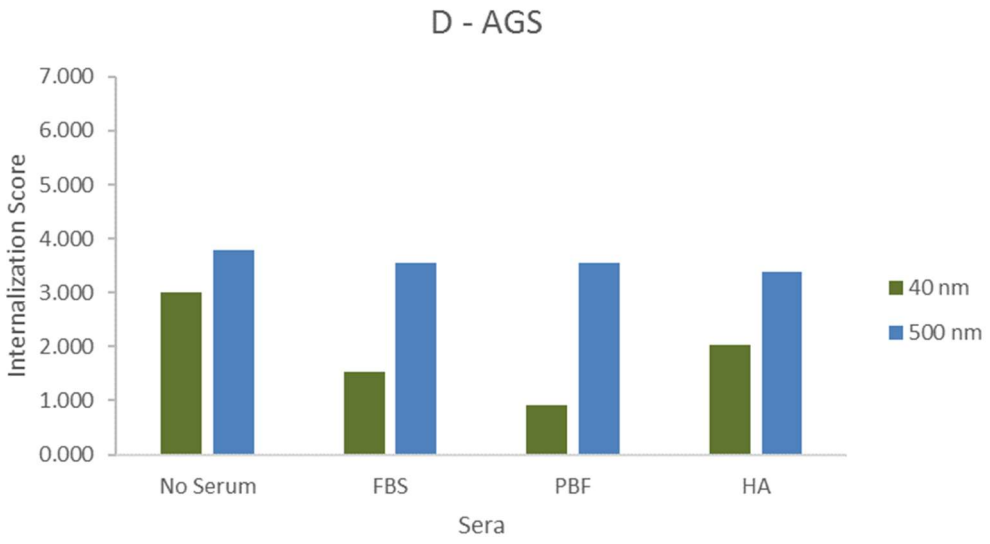
D - AGS
Internalization Score
7.000
6.000
5.000
4.000
3.000
2.000
1.000
0.000
No Serum
FBS
PBF
HA
Sera
40 nm
500 nm

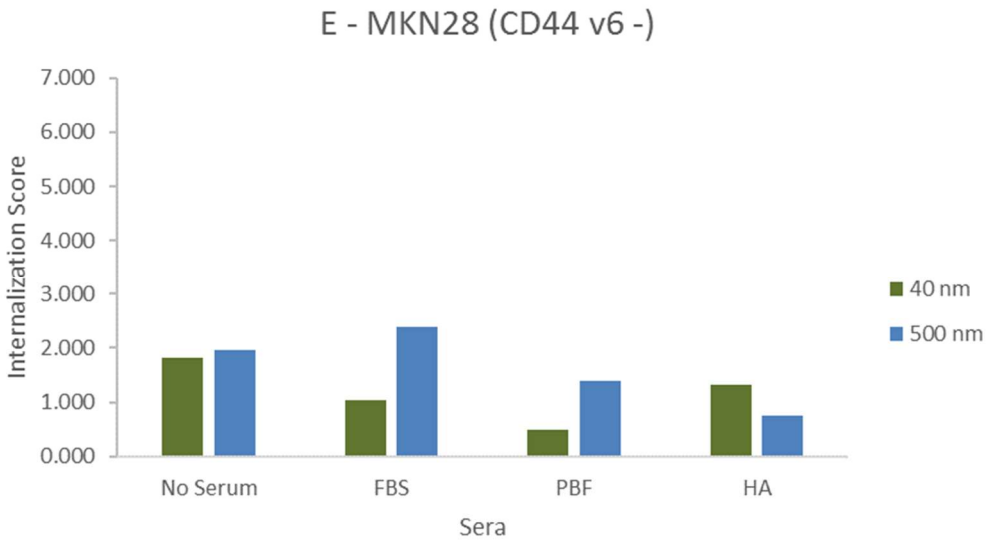
E - MKN28 (CD44 v6 -)
Internalization Score
7.000
6.000
5.000
4.000
3.000
2.000
1.000
0.000
No Serum
FBS
PBF
HA
Sera
40 nm
500 nm

Figure 7 - Influence of NP size and protein corona on the NPs uptake (during 24h) across various cell lines, as assessed by imaging flow cytometry. (A) Hek293t cell line; (B) HeLa cell line; (C) GP202 cell line; (D) AGS cell line; (E) MKN28 cell line. Results are reported as median value of the internalization score of NPs uptake taking in consideration the internalization feature of the IDEAS software

The preliminary results obtained through imaging flow cytometry, and comparing with those performed previously by flow cytometry, confirm the previous behavior observed for the 40 nm NPs, namely a lower internalization in the “PBF” condition, compared to the “No serum” condition. However, the increased uptake of 500 nm particles in the same condition, was not verified, at least to the same level found by flow cytometry. In this later case, as shown in Fig. S4, the signal from NPs was shown to be saturated (throughout all serum conditions) and there were barely any differences in the internalization score of 500 nm particles among all cell lines (Fig. 7), indicating that additional experiments and new settings need to be optimized in order to better correlate both techniques. A possible way to decrease the obtained signal saturation, could pass through using a lower concentration of NPs in the incubation solution, or different instrument settings could be used to analyze the 40 and 500 nm NPs.

According to the results presented in Fig. 7, the cell line with the biggest uptake of 40 and 500 nm NPs was the HeLa cells (except in the uptake of 40 nm NPs with a protein corona derived from PBF). This wasn’t expected, since the previous results (Fig. 4B and C) obtained through flow cytometry indicated that there was a more substantial NPs uptake in the GP202 cell line, when compared to the HeLa cell line. The reason for this could be due to the complexity and additional gating presented in the internalization score calculation, which needs to be optimized.

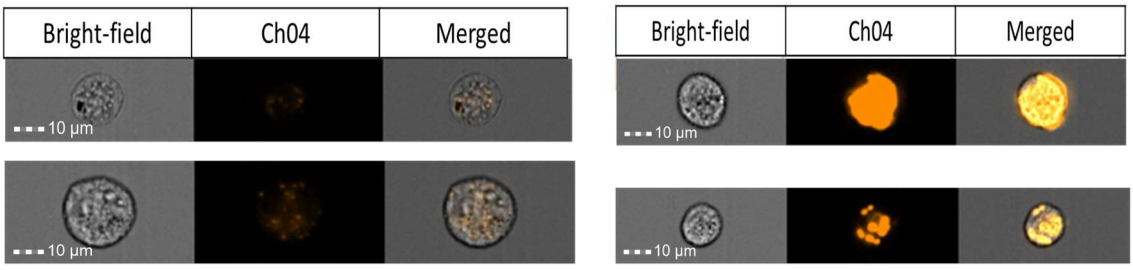

Figure 8 - Comparison of the uptake of 40 nm NPs, in medium supplemented with PBF, in two AGS cells (left images) with the uptake of 500 nm NPs, in medium without serum, also in two AGS cells (right images).

Other issues that require further optimization were detected when exploring imaging flow cytometry for the current purpose. The instrument settings used were the same for the analysis of all samples and they correspond to the lowest intensity power

possible (488 nm laser power: 10.00; 785 nm laser power: 11.00). But even with such low intensity, cells with a very high uptake of either sized NPs, had their signal saturated. Even 40 nm NPs, which possessed lower fluorescence than 500 nm NPs, had their signal saturated in cases of a very high uptake, as it can be seen in Fig. S4A, B and D. On the other hand, the 40 nm NPs, incubated in media supplemented in "PBF" serum, were difficult to be visualized, due to their lower uptake and the used settings (Figs. S4 C). Nonetheless, a smaller uptake of these particles was verified, when compared with same-sized particles incubated in SFM, which was one of the intended goals of these first experiences. It can also be noticed in Table S4 that, even though the equipment was set to acquire 10 000 cells, the cell count is not exactly 10 000 cells. This is due to interruption in the flow when the equipment stops acquiring events, and some cells may be removed and neglected or taken into consideration, depending on their morphology. Also, more than half of the cells acquired are not used in the calculation of the median (Table S4 and explained in Fig. S3). Additional experiments will be needed to confirm the internalization score results obtained in imaging flow cytometry.

Looking at the merged images of Fig. 8 and Fig. S3, the nanoparticles were clearly located throughout the cytoplasm, but to infer more information than that is very difficult. The Imagestream is also capable of analyzing more fluorophores and it is especially used for co-localization assays as well, through the use of the co-localization feature of the IDEAS software, and for counting NPs, through the spot count feature of the same software. Both features are able to significantly contribute to the quantity and location of NPs within a cell.[143, 144]

It should be noted that most of the work consisted in *in vitro* experiments and using cell culture models. Such approach was selected because there is very little information about the effects/consequences of protein adsorption on nanoparticles *in vivo*. This is due to the complexity of the *in vivo* situation since, after intravenous injection of nanoparticles in a living organism, these will almost immediately form their respective protein coronas throughout the circulatory system, facing billions of moving cells and the large surface area of the vascular endothelial cells, making it very difficult a study similar to the present one.[102]

5. Conclusions and Perspectives

In summary, the cell uptake profile of NPs is dependent of the NPs size, the proteins absorbed to the NP surface, and the type of cells studied, confirming the complexity of endocytosis of NPs by cells. More importantly, the data obtained in this work highlights that smaller NPs, when exhibiting a PBF-originated protein corona, are less uptaken by cells, when compared to equally-sized NPs in SFM. On the contrary, larger NPs, that present the PBF-originated corona, resulted in an increasingly high uptake by cells, when compared to same-sized NPs in the SFM. Understanding the reason for this change in the uptake, could lead to a better understanding of endocytosis and, consequently, to possibly new drug delivery techniques in nanomedicine.

Future work includes the continuation of the NPs uptake experiments, expanding to other cell lines, like the SW892 synovial fibroblast cell line, to see if the tendency demonstrated by the PBF condition remains. It would also be interesting to test how NPs uptake would play out in different types of primary cells.

The detailed study of the PBF serum and the composition of the protein corona, through western blots and proteomics are also extremely important to explain the differences observed in the protein coronas formed. It can also lead to potential new uses for the PBF serum. Time profiles of the NPs uptake experiments should be repeated in all the cell lines.

Finally, the use of imaging flow cytometry to characterize NPs internalization by cells should be further explored and optimized, especially to allow detection of NP localization. The cell lines tested here and the differently sized NPs should also be included in forthcoming studies. The spot count and the co-localization features of the Imagestream constitute powerful tools that should be further explored, to determine the final localization of the NPs within the cell.

6. References

[1] Liu, Y., Miyoshi, H., and Nakamura, M. (2007) Nanomedicine for drug delivery and imaging: a promising avenue for cancer therapy and diagnosis using targeted functional nanoparticles, *Int. J. Cancer 120*, 2527-2537.

[2] Whitesides, G. M. (2005) Nanoscience, nanotechnology, and chemistry, *Small 1*, 172-179.

[3] Thrall, J. H. (2004) Nanotechnology and Medicine, *Radiology 230*, 315-318.

[4] Langer, R., and Weissleder, R. (2015) Nanotechnology, *J. A. M. A. 313*, 135-136.

[5] Duncan, R., and Vicent, M. J. (2013) Polymer therapeutics-prospects for 21st century: the end of the beginning, *Adv. Drug Deliv. Rev. 65*, 60-70.

[6] Couvreur, P., Couarraze, G., Devissaguet, J.-P., and Puisieux, F. (1996) Nanoparticles: preparation and characterization, In *Microencapsulation: Methods and Industrial Application* (Benita, S., Ed.), pp 183-211, Marcel Dekker, New York.

[7] Albanese, A., Tang, P. S., and Chan, W. C. (2012) The effect of nanoparticle size, shape, and surface chemistry on biological systems, *Annu. Rev. Biomed. Eng. 14*, 1-16.

[8] Prasad Shastri, V. (2003) Non-degradable biocompatible polymers in medicine: Past, present and future, *Curr. Pharm. Biotechn. 4*, 331-337.

[9] Burman, A. C., Mukherjee, R., Khattar, D., Mullick, S., Jaggi, M., Singh, M. K., Kumar, M., Prusthy, D., Gupta, P. K., and Praveen, R. (2015) Biocompatible, non-biodegradable, non-toxic polymer useful for nanoparticle pharmaceutical compositions.

[10] Truong, N. P., Whittaker, M. R., Mak, C. W., and Davis, T. P. (2015) The importance of nanoparticle shape in cancer drug delivery, *Expert Opin. Drug Deliv. 12*, 129-142.

[11] Schutz, C. A., Juillerat-Jeanneret, L., Mueller, H., Lynch, I., and Riediker, M. (2013) Therapeutic nanoparticles in clinics and under clinical evaluation, *Nanomedicine 8*, 449-467.

[12] Banik, B. L., Fattahi, P., and Brown, J. L. (2016) Polymeric nanoparticles: the future of nanomedicine, *Wiley Interdiscip. Rev. Nanomed. Nanobiotechnol. 8*, 271-299.

[13] Hanahan, D., and Weinberg, R. A. (2000) The Hallmarks of Cancer, *Cell 100*, 57-70.

[14] Hanahan, D., and Weinberg, R. A. (2011) Hallmarks of cancer: the next generation, *Cell 144*, 646-674.

[15] Links, M., and Brown, R. (1999) Clinical relevance of the molecular mechanisms of resistance to anti-cancer drugs, *Expert Rev. Mol. Med. 1999*, 1-21.

[16] Perez-Herrero, E., and Fernandez-Medarde, A. (2015) Advanced targeted therapies in cancer: Drug nanocarriers, the future of chemotherapy, *Eur. J. Pharm. Biopharm. 93*, 52-79.

[17] Brannon-Peppas, L., and Blanchette, J. O. (2012) Nanoparticle and targeted systems for cancer therapy, *Adv. Drug Deliv. Rev. 64*, 206-212.

[18] Northfelt, D. W., Martin, F. J., Working, P., Volberding, P. A., Russell, J., Newman, M., Amantea, M. A., and Kaplan, L. D. (1996) Doxorubicin encapsulated in liposomes containing surface-bound polyethylene glycol: Pharmacokinetics, tumor localization, and safety in patients with AIDS-related Kaposi's sarcoma, *J. Clin. Pharmacol. 36*, 55-63.

[19] Iyer, A. K., Khaled, G., Fang, J., and Maeda, H. (2006) Exploiting the enhanced permeability and retention effect for tumor targeting, *Drug Discov. Today 11*, 812-818.

[20] Danhier, F., Feron, O., and Preat, V. (2010) To exploit the tumor microenvironment: Passive and active tumor targeting of nanocarriers for anti-cancer drug delivery, *J. Control. Release 148*, 135-146.

[21] Maeda, H. (2001) The enhanced permeability and retention (EPR) effect in tumor vasculature: The key role of tumor-selective macromolecular drug targeting, In *Adv. Enzyme Regul.*, pp 189-207.

[22] Iversen, T.-G., Skotland, T., and Sandvig, K. (2011) Endocytosis and intracellular transport of nanoparticles: Present knowledge and need for future studies, *Nano Today 6*, 176-185.

[23] Aderem, A., and Underhill, D. M. (1999) Mechanism of Phagocytosis in Macrophages, *Annu. Rev. Immunol. 17*, 593-623.

[24] Popova, N. V., Deyev, I. E., and Petrenko, A. G. (2013) Clathrin-mediated Endocytosis and Adaptor Proteins, *Acta Naturae 5*, 62-73.

[25] Huang, F., Khvorova, A., Marshall, W., and Sorkin, A. (2004) Analysis of Clathrin-mediated Endocytosis of Epidermal Growth Factor Receptor by RNA Interference, *J. Biol. Chem. 279*, 16657-16661.

[26] Granseth, B., Odermatt, B., Royle, S., and Lagnado, L. (2006) Clathrin-Mediated Endocytosis Is the Dominant Mechanism of Vesicle Retrieval at Hippocampal Synapses, *Neuron 51*, 773-786.

[27] Rejman, J., Oberle, V., Zuhorn, I. S., and Hoekstra, D. (2004) Size-dependent internalization of particles via the pathways of clathrin-and caveolae-mediated endocytosis, *Biochem. J. 377*, 159-169.

[28] Orlandi, P. A., and Fishman, P. H. (1998) Filipin-dependent inhibition of cholera toxin: Evidence for toxin internalization and activation through caveolae-like domains, *J. Cell Biol. 141*, 905-915.

[29] Damm, E. M., Pelkmans, L., Kartenbeck, J., Mezzacasa, A., Kurzchalia, T., and Helenius, A. (2005) Clathrin- and caveolin-1-independent endocytosis: Entry of simian virus 40 into cells devoid of caveolae, *J. Cell Biol. 168*, 477-488.

[30] Simons, K., and Toomre, D. (2000) Lipid rafts and signal transduction, *Nat. Rev. Mol. Cell Bio. 1*, 31-39.

[31] Alonso, M. A., and Millán, J. (2001) The role of lipid rafts in signalling and membrane trafficking in T lymphocytes, *J. Cell Sci. 114*, 3957-3965.

[32] Conner, S. D., and Schmid, S. L. (2003) Regulated portals of entry into the cell, *Nature 422*, 37-44.

[33] Nabi, I. R., and Le, P. U. (2003) Caveolae/raft-dependent endocytosis, *J. Cell Biol. 161*, 673-677.

[34] Swanson, J. A., and Watts, C. (1995) Macropinocytosis, *Trends Cell Biol. 5*, 424-428.

[35] Mercer, J., and Helenius, A. (2009) Virus entry by macropinocytosis, *Nat. Cell Biol. 11*, 510-520.

[36] Rao, J. P., and Geckeler, K. E. (2011) Polymer nanoparticles: Preparation techniques and size-control parameters, *Prog. Polym. Sci. 36*, 887-913.

[37] Mitragotri, S., and Lahann, J. (2009) Physical approaches to biomaterial design, *Nat. Mat. 8*, 15-23.

[38] Shang, L., Nienhaus, K., and Nienhaus, G. U. (2014) Engineered nanoparticles interacting with cells-size matters, *J. Nanobiotechnol. 12*.

[39] Shang, W., Nuffer, J. H., Muñiz-Papandrea, V. A., Colón, W., Siegel, R. W., and Dordick, J. S. (2009) Cytochrome c on silica nanoparticles: Influence of nanoparticle size on protein structure, stability, and activity, *Small 5*, 470-476.

[40] Tenzer, S., Docter, D., Rosfa, S., Wlodarski, A., Kuharev, J., Rekik, A., Knauer, S. K., Bantz, C., Nawroth, T., Bier, C., Sirirattanapan, J., Mann, W., Treuel, L., Zellner, R., Maskos, M., Schild, H., and Stauber, R. H. (2011) Nanoparticle size is a critical physicochemical determinant of the human blood plasma corona: A comprehensive quantitative proteomic analysis, *ACS Nano 5*, 7155-7167.

[41] Wang, J., Jensen, U. B., Jensen, G. V., Shipovskov, S., Balakrishnan, V. S., Otzen, D., Pedersen, J. S., Besenbacher, F., and Sutherland, D. S. (2011) Soft interactions at nanoparticles alter protein function and conformation in a size dependent manner, *Nano Lett. 11*, 4985-4991.

[42] Tenzer, S., Docter, D., Kuharev, J., Musyanovych, A., Fetz, V., Hecht, R., Schlenk, F., Fischer, D., Kiouptsi, K., Reinhardt, C., Landfester, K., Schild, H., Maskos, M., Knauer, S. K., and Stauber, R. H. (2013) Rapid formation of plasma protein corona critically affects nanoparticle pathophysiology, *Nat. Nanotechnol. 8*, 772-781.

[43] He, C., Hu, Y., Yin, L., Tang, C., and Yin, C. (2010) Effects of particle size and surface charge on cellular uptake and biodistribution of polymeric nanoparticles, *Biomaterials 31*, 3657-3666.

[44] Win, K. Y., and Feng, S. S. (2005) Effects of particle size and surface coating on cellular uptake of polymeric nanoparticles for oral delivery of anticancer drugs, *Biomaterials 26*, 2713-2722.

[45] Verma, A., and Stellacci, F. (2010) Effect of surface properties on nanoparticle-cell interactions, *Small 6*, 12-21.

[46] Kulkarni, S. A., and Feng, S. S. (2013) Effects of particle size and surface modification on cellular uptake and biodistribution of polymeric nanoparticles for drug delivery, *Pharm. Res. 30*, 2512-2522.

[47] Tan, J., Shah, S., Thomas, A., Ou-Yang, H. D., and Liu, Y. (2013) The influence of size, shape and vessel geometry on nanoparticle distribution, *Microfluid. Nanofluidics 14*, 77-87.

[48] Townson, J. L., Lin, Y. S., Agola, J. O., Carnes, E. C., Leong, H. S., Lewis, J. D., Haynes, C. L., and Brinker, C. J. (2013) Re-examining the size/charge paradigm: differing in vivo characteristics of size- and charge-matched mesoporous silica nanoparticles, *J. Am. Chem. Soc. 135*, 16030-16033.

[49] Mironava, T., Hadjiargyrou, M., Simon, M., Jurukovski, V., and Rafailovich, M. H. (2010) Gold nanoparticles cellular toxicity and recovery: Effect of size, concentration and exposure time, *Nanotoxicology 4*, 120-137.

[50] Chithrani, B. D., Ghazani, A. A., and Chan, W. C. W. (2006) Determining the size and shape dependence of gold nanoparticle uptake into mammalian cells, *Nano Lett. 6*, 662-668.

[51] Alexis, F., Pridgen, E., Molnar, L. K., and Farokhzad, O. C. (2008) Factors affecting the clearance and biodistribution of polymeric nanoparticles, *Mol. Pharm. 5*, 505-515.

[52] Tang, L., Yang, X., Yin, Q., Cai, K., Wang, H., Chaudhury, I., Yao, C., Zhou, Q., Kwon, M., Hartman, J. A., Dobrucki, I. T., Dobrucki, L. W., Borst, L. B., Lezmi, S., Helferich, W. G., Ferguson, A. L., Fan, T. M., and Cheng, J. (2014) Investigating the optimal size of anticancer nanomedicine, *Proc. Natl. Acad. Sci. U. S. A. 111*, 15344-15349.

[53] Elsabahy, M., and Wooley, K. L. (2012) Design of polymeric nanoparticles for biomedical delivery applications, *Chem. Soc. Rev. 41*, 2545-2561.

[54] Petros, R. A., and Desimone, J. M. (2010) Strategies in the design of nanoparticles for therapeutic applications, *Nat. Rev. Drug Discov. 9*, 615-627.

[55] Moghimi, S. M., Hunter, A. C., and Murray, J. C. (2005) Nanomedicine: Current status and future prospects, *FASEB Journal 19*, 311-330.

[56] Swami, A., Shi, J., Gadde, S., Votruba, A. R., Kolishetti, N., and Farokhzad, O. C. (2012) Nanoparticles for targeted and temporally controlled drug delivery, In *Multifunctional Nanoparticles for Drug Delivery Applications* (Svenson, S., and Prud'homme, R. K., Eds.), pp 9-29, Springer.

[57] Duchene, D., and Gref, R. (2016) Small is beautiful: Surprising nanoparticles, *Int. J. Pharm. 502*, 219-231.

[58] Doane, T. L., and Burda, C. (2012) The unique role of nanoparticles in nanomedicine: imaging, drug delivery and therapy, *Chem. Soc. Rev. 41*, 2885-2911.

[59] Christian, D. A., Cai, S., Garbuzenko, O. B., Harada, T., Zajac, A. L., Minko, T., and Discher, D. E. (2009) Flexible filaments for in vivo imaging and delivery: Persistent circulation of filomicelles opens the dosage window for sustained tumor shrinkage, *Molec. Pharm. 6*, 1343-1352.

[60] Mitragotri, S. (2009) In drug delivery, shape does matter, *Pharm. Res. 26*, 232-234.

[61] Champion, J. A., Katare, Y. K., and Mitragotri, S. (2007) Making polymeric micro- and nanoparticles of complex shapes, *Proc. Natl. Acad. Sci. U. S. A. 104*, 11901-11904.

[62] Park, J. G., Forster, J. D., and Dufresne, E. R. (2010) High-yield synthesis of monodisperse dumbbell-shaped polymer nanoparticles, *J. Am. Chem. Soc. 132*, 5960-5961.

[63] Doshi, N., Zahr, A. S., Bhaskar, S., Lahann, J., and Mitragotri, S. (2009) Red blood cell-mimicking synthetic biomaterial particles, *Proc. Natl. Acad. Sci. U. S. A. 106*, 21495-21499.

[64] Champion, J. A., Katare, Y. K., and Mitragotri, S. (2007) Particle shape: A new design parameter for micro- and nanoscale drug delivery carriers, *J. Control. Release 121*, 3-9.

[65] He, J., Perez, M. T., Zhang, P., Liu, Y., Babu, T., Gong, J., and Nie, Z. (2012) A general approach to synthesize asymmetric hybrid nanoparticles by interfacial reactions, *J. Am. Chem. Soc. 134*, 3639-3642.

[66] Tao, L., Hu, W., Liu, Y., Huang, G., Sumer, B. D., and Gao, J. (2011) Shape-specific polymeric nanomedicine: emerging opportunities and challenges, *Exp. Biol. Med. 236*, 20-29.

[67] Dasgupta, S., Auth, T., and Gompper, G. (2014) Shape and orientation matter for the cellular uptake of nonspherical particles, *Nano Lett. 14*, 687-693.

[68] Gratton, S. E., Ropp, P. A., Pohlhaus, P. D., Luft, J. C., Madden, V. J., Napier, M. E., and DeSimone, J. M. (2008) The effect of particle design on cellular internalization pathways, *Proc. Natl. Acad. Sci. U. S. A. 105*, 11613-11618.

[69] Geng, Y., Dalhaimer, P., Cai, S., Tsai, R., Tewari, M., Minko, T., and Discher, D. E. (2007) Shape effects of filaments versus spherical particles in flow and drug delivery, *Nature Nanotech. 2*, 249-255.

[70] Gabizon, A., Shmeeda, H., and Barenholz, Y. (2003) Pharmacokinetics of pegylated liposomal doxorubicin: Review of animal and human studies, *Clinical Pharmacokinetics 42*, 419-436.

[71] Dalhaimer, P., Engler, A. J., Parthasarathy, R., and Discher, D. E. (2004) Targeted worm micelles, *Biomacromolecules 5*, 1714-1719.

[72] Arnida, Janát-Amsbury, M. M., Ray, A., Peterson, C. M., and Ghandehari, H. (2011) Geometry and surface characteristics of gold nanoparticles influence their biodistribution and uptake by macrophages, *Eur. J. Pharm. Biopharm. 77*, 417-423.

[73] Zhou, Z., Ma, X., Jin, E., Tang, J., Sui, M., Shen, Y., Van Kirk, E. A., Murdoch, W. J., and Radosz, M. (2013) Linear-dendritic drug conjugates forming long-circulating nanorods for cancer-drug delivery, *Biomaterials 34*, 5722-5735.

[74] Ma, N., Ma, C., Li, C., Wang, T., Tang, Y., Wang, H., Mou, X., Chen, Z., and He, N. (2013) Influence of nanoparticle shape, size, and surface functionalization on cellular uptake, *J. Nanosci. Nanotechnol. 13*, 6485-6498.

[75] Schick, I., Lorenz, S., Storck, W., Fischer, K., Strand, D., Laqai, F., and Tremel, W. (2014) Inorganic Janus particles for biomedical applications, *Belstein J. Nanotechnol. 5*, 2346-2362.

[76] Perro, A., Reculusa, S., Ravaine, S., Bourgeat-Lami, E., and Duguet, E. (2005) Design and synthesis of Janus micro- and nanoparticles, *J. Mater. Chem. 15*, 3745-3760.

[77] Voets, I. K., De Keizer, A., De Waard, P., Frederik, P. M., Bomans, P. H. H., Schmalz, H., Walther, A., King, S. M., Leermakers, F. A. M., and Cohen Stuart, M. A. (2006) Double-faced micelles from water-soluble polymers, *Angew. Chem. Int. Ed. 45*, 6673-6676.

[78] Cheng, L., Zhang, G., Zhu, L., Chen, D., and Jiang, M. (2008) Nanoscale tubular and sheetlike superstructures from hierarchical self-assembly of polymeric Janus particles, *Angewandte Chemie - International Edition 47*, 10171-10174.

[79] Tran, L. T. C., Lesieur, S., and Faivre, V. (2014) Janus nanoparticles: Materials, preparation and recent advances in drug delivery, *Expert Opin. Drug Deliv. 11*, 1061-1074.

[80] Shao, D., Li, J., Zheng, X., Pan, Y., Wang, Z., Zhang, M., Chen, Q.-X., Dong, W.-F., and Chen, L. (2016) Janus “nano-bullets” for magnetic targeting liver cancer chemotherapy, *Biomaterials 100*, 118-133.

[81] Cedervall, T., Lynch, I., Lindman, S., Berggard, T., Thulin, E., Nilsson, H., Dawson, K. A., and Linse, S. (2007) Understanding the nanoparticle-protein corona using methods to quantify exchange rates and affinities of proteins for nanoparticles, *Proc. Natl. Acad. Sci. U. S. A. 104*, 2050-2055.

[82] Klein, J. (2007) Probing the interactions of proteins and nanoparticles, *Proc. Natl. Acad. Sci. U. S. A. 104*, 2029-2030.

[83] Watson, P., Jones, A. T., and Stephens, D. J. (2005) Intracellular trafficking pathways and drug delivery: fluorescence imaging of living and fixed cells, *Adv. Drug Deliv. Rev. 57*, 43-61.

[84] Chithrani, B. D., and Chan, W. C. W. (2007) Elucidating the mechanism of cellular uptake and removal of protein-coated gold nanoparticles of different sizes and shapes, *Nano Lett. 7*, 1542-1550.

[85] Jiang, W., Kim, B. Y. S., Rutka, J. T., and Chan, W. C. W. (2008) Nanoparticle-mediated cellular response is size-dependent, *Nat. Nanotechnol. 3*, 145-150.

[86] Hellstrand, E., Lynch, I., Andersson, A., Drakenberg, T., Dahlbäck, B., Dawson, K. A., Linse, S., and Cedervall, T. (2009) Complete high-density lipoproteins in nanoparticle corona, *FEBS 276*, 3372-3381.

[87] Nel, A. E., Mädler, L., Velegol, D., Xia, T., Hoek, E. M. V., Somasundaran, P., Klaessig, F., Castranova, V., and Thompson, M. (2009) Understanding biophysicochemical interactions at the nano-bio interface, *Nat. Mater. 8*, 543-557.

[88] Dell'Orco, D., Lundqvist, M., Oslakovic, C., Cedervall, T., and Linse, S. (2010) Modeling the time evolution of the nanoparticle-protein corona in a body fluid, *PLoS ONE 5*.

[89] Monopoli, M. P., Walczyk, D., Campbell, A., Elia, G., Lynch, I., Baldelli Bombelli, F., and Dawson, K. A. (2011) Physical-Chemical aspects of protein corona: Relevance to in vitro and in vivo biological impacts of nanoparticles, *J. Am. Chem. Soc. 133*, 2525-2534.

[90] Caracciolo, G., Pozzi, D., Candeloro De Sanctis, S., Laura Capriotti, A., Caruso, G., Samperi, R., and Laganà, A. (2011) Effect of membrane charge density on the protein corona of cationic liposomes: Interplay between cationic charge and surface area, *Applied Physics Letters 99*.

[91] Gräfe, C., Weidner, A., Lühe, M. V. D., Bergemann, C., Schacher, F. H., Clement, J. H., and Dutz, S. (2016) Intentional formation of a protein corona on nanoparticles: Serum concentration affects protein corona mass, surface charge, and nanoparticle-cell interaction, *International Journal of Biochemistry and Cell Biology 75*, 196-202.

[92] Lundqvist, M., Stigler, J., Elia, G., Lynch, I., Cedervall, T., and Dawson, K. A. (2008) Nanoparticle size and surface properties determine the protein corona with possible implications for biological impacts, *Proc. Natl. Acad. Sci. U. S. A. 105*, 14265-14270.

[93] Lynch, I., and Dawson, K. A. (2008) Protein-nanoparticle interactions, *Nano Today 3*, 40-47.

[94] Ehrenberg, M. S., Friedman, A. E., Finkelstein, J. N., Oberdörster, G., and McGrath, J. L. (2009) The influence of protein adsorption on nanoparticle association with cultured endothelial cells, *Biomaterials 30*, 603-610.

[95] Mu, Q., Li, Z., Li, X., Mishra, S. R., Zhang, B., Si, Z., Yang, L., Jiang, W., and Yan, B. (2009) Characterization of Protein Clusters of Diverse Magnetic Nanoparticles and Their Dynamic Interactions with Human Cells, *J. Phys. Chem. C. 113*, 5390-5395.

[96] Simberg, D., Park, J. H., Karmali, P. P., Zhang, W. M., Merkulov, S., McCrae, K., Bhatia, S. N., Sailor, M., and Ruoslahti, E. (2009) Differential proteomics analysis of the surface heterogeneity of dextran iron oxide nanoparticles and the implications for their in vivo clearance, *Biomaterials 30*, 3926-3933.

[97] Cedervall, T., Lynch, I., Foy, M., Berggård, T., Donnelly, S. C., Cagney, G., Linse, S., and Dawson, K. A. (2007) Detailed identification of plasma proteins adsorbed on copolymer nanoparticles, *Angew. Chem. Int. Ed. 46*, 5754-5756.

[98] El-Ansary, A., and Al-Daihan, S. (2009) On the toxicity of therapeutically used nanoparticles: an overview, *J. Toxicol. 2009*, 754810.

[99] Walczyc, D., Bombelli, F. B., Monopoli, M. P., Lynch, I., and Dawson, K. A. (2009) What the Cell "Sees" in Bionanoscience, *J. Am. Chem. Soc.. 132*, 5761-5768.

[100] Larson, T. A., Joshi, P. P., and Sokolov, K. (2012) Preventing protein adsorption and macrophage uptake of gold nanoparticles via a hydrophobic shield, *ACS Nano 6*, 9182-9190.

[101] Walkey, C. D., and Chan, W. C. W. (2012) Understanding and controlling the interaction of nanomaterials with proteins in a physiological environment, *Chem. Soc. Rev. 41*, 2780-2799.

[102] Bargheer, D., Nielsen, J., Gebel, G., Heine, M., Salmen, S. C., Stauber, R., Weller, H., Heeren, J., and Nielsen, P. (2015) The fate of a designed protein corona on nanoparticles in vitro and in vivo, *Beilstein J. Nanotechnol. 6*, 36-46.

[103] Milani, S., Baldelli Bombelli, F., Pitek, A. S., Dawson, K. A., and Rädler, J. (2012) Reversible versus irreversible binding of transferrin to polystyrene nanoparticles: Soft and hard corona, *ACS Nano 6*, 2532-2541.

[104] Lynch, I., Salvati, A., and Dawson, K. A. (2009) Protein-nanoparticle interactions: What does the cell see?, *Nat. Nanotechnol. 4*, 546-547.

[105] Martel, J., Young, D., Young, A., Wu, C.-Y., Chen, C.-D., Yu, J.-S., and Young, J. D. (2011) Comprehensive proteomic analysis of mineral nanoparticles derived from human body fluids and analyzed by liquid chromatography–tandem mass spectrometry, *Anal. Biochem. 418*, 111-125.

[106] Dobrovolskaia, M. A., Patri, A. K., Zheng, J., Clogston, J. D., Ayub, N., Aggarwal, P., Neun, B. W., Hall, J. B., and McNeil, S. E. (2009) Interaction of colloidal gold nanoparticles with human blood: effects on particle size and analysis of plasma protein binding profiles, *Nanomedicine 5*, 106-117.

[107] Zhang, H., Burnum, K. E., Luna, M. L., Petritis, B. O., Kim, J.-S., Qian, W.-J., Moore, R. J., Heredia-Langner, A., Webb-Robertson, B.-J. M., Thrall, B. D., Camp, D. G., Smith, R. D., Pounds, J. G., and Liu, T. (2011) Quantitative proteomics analysis of adsorbed plasma proteins classifies nanoparticles with different surface properties and size, *PROTEOMICS 11*, 4569-4577.

[108] Maiorano, G., Sabella, S., Sorce, B., Brunetti, V., Malvindi, M. A., Cingolani, R., and Pompa, P. P. (2010) Effects of Cell Culture Media on the Dynamic Formation of Protein−Nanoparticle Complexes and Influence on the Cellular Response, *ACS Nano 4*, 7481-7491.

[109] Sund, J., Alenius, H., Vippola, M., Savolainen, K., and Puustinen, A. (2011) Proteomic Characterization of Engineered Nanomaterial–Protein Interactions in Relation to Surface Reactivity, *ACS Nano 5*, 4300-4309.

[110] Schaefer, J., Schulze, C., Marxer, E. E. J., Schaefer, U. F., Wohlleben, W., Bakowsky, U., and Lehr, C.-M. (2012) Atomic Force Microscopy and Analytical Ultracentrifugation for Probing Nanomaterial Protein Interactions, *ACS Nano 6*, 4603-4614.

[111] Zheng, M., Li, Z., and Huang, X. (2004) Ethylene Glycol Monolayer Protected Nanoparticles: Synthesis, Characterization, and Interactions with Biological Molecules, *Langmuir 20*, 4226-4235.

[112] Zhou, J. D., Gysell, M., Tara, S., Anthony, M., Darren, M., and Rodney, F. M. (2009) Differential plasma protein binding to metal oxide nanoparticles, *Nanotechnology 20*, 455101.

[113] Wang, B., Zhang, L., Sung, C. B., and Granick, S. (2008) Nanoparticle-induced surface reconstruction of phospholipid membranes, *Proc. Natl. Acad. Sci. U. S. A. 105*, 18171-18175.

[114] Dawson, K. A., Salvati, A., and Lynch, I. (2009) Nanotoxicology: Nanoparticles reconstruct lipids, *Nat. Nanotechnol. 4*, 84-85.

[115] Mahmoudi, M., Meng, J., Xue, X., Liang, X. J., Rahman, M., Pfeiffer, C., Hartmann, R., Gil, P. R., Pelaz, B., Parak, W. J., Del Pino, P., Carregal-Romero, S., Kanaras, A. G., and Tamil Selvan, S. (2014) Interaction of stable colloidal nanoparticles with cellular membranes, *Biotech. Adv. 32*, 679-692.

[116] Gagner, J. E., Shrivastava, S., Qian, X., Dordick, J. S., and Siegel, R. W. (2012) Engineering Nanomaterials for Biomedical Applications Requires Understanding the Nano-Bio Interface: A Perspective, *J. Phys. Chem. Lett. 3*, 3149-3158.

[117] Elsaesser, A., and Howard, C. V. (2012) Toxicology of nanoparticles, *Adv. Drug Deliv. Rev. 64*, 129-137.

[118] Mahmoudi, M., Saeedi-Eslami, S. N., Shokrgozar, M. A., Azadmanesh, K., Hassanlou, M., Kalhor, H. R., Burtea, C., Rothen-Rutishauser, B., Laurent, S., Sheibani, S., and Vali, H. (2012) Cell "vision": Complementary factor of protein corona in nanotoxicology, *Nanoscale 4*, 5461-5468.

[119] Barua, S., and Rege, K. (2009) Cancer-cell-phenotype-dependent differential intracellular trafficking of unconjugated quantum dots, *Small 5*, 370-376.

[120] Gur, G., and Yarden, Y. (2004) Enlightened receptor dynamics, *Nat. Biotechnol. 22*, 169-170.

[121] Kaplan, J. (1976) Cell contact induces an increase in pinocytotic rate in cultured epithelial cells, *Nature 263*, 596-597.

[122] Snijder, B., Sacher, R., Rämö, P., Damm, E. M., Liberali, P., and Pelkmans, L. (2009) Population context determines cell-to-cell variability in endocytosis and virus infection, *Nature 461*, 520-523.

[123] da Cunha, C. B., Oliveira, C., Wen, X., Gomes, B., Sousa, S., Suriano, G., Grellier, M., Huntsman, D. G., Carneiro, F., Granja, P. L., and Seruca, R. (2010) De novo expression of CD44 variants in sporadic and hereditary gastric cancer, *Lab. Invest. 90*, 1604-1614.

[124] Branco da Cunha, C., Klumpers, D. D., Koshy, S. T., Weaver, J. C., Chaudhuri, O., Seruca, R., Carneiro, F., Granja, P. L., and Mooney, D. J. (2016) CD44 alternative splicing in gastric cancer cells is regulated by culture dimensionality and matrix stiffness, *Biomaterials 98*, 152-162.

[125] Aruffo, A., Stamenkovic, I., Melnick, M., Underhill, C. B., and Seed, B. (1990) CD44 is the principal cell surface receptor for hyaluronate, *Cell 61*, 1303-1313.

[126] Ayhan, A., Tok, E. C., Bildirici, I., and Ayhan, A. (2001) Overexpression of CD44 variant 6 in human endometrial cancer and its prognostic significance, *Gynecol. Oncol. 80*, 355-358.

[127] Borland, G., Ross, J. A., and Guy, K. (1998) Forms and functions of CD44, *Immunology 93*, 139-148.

[128] Castella, E. M., Ariza, A., Ojanguren, I., Mate, J. L., Roca, X., Fernandez-Vasalo, A., and Navas-Palacios, J. J. (1996) Differential expression of CD44v6 in adenocarcinoma of the pancreas: an immunohistochemical study, *Virchows Arch. 429*, 191-195.

[129] Clarke, G., Ryan, E., O'Keane, J. C., Crowe, J., and Mathúna, P. M. (2000) Mortality association of enhanced CD44v6 expression is not mediated through occult lymphatic spread in stage II colorectal cancer, *J. of Gastroen and Hepatol. 15*, 1028-1031.

[130] (2016) Orthosera, http://www.orthosera.com/en/group.

[131] dos Santos, T., Varela, J., Lynch, I., Salvati, A., and Dawson, K. A. (2011) Effects of transport inhibitors on the cellular uptake of carboxylated polystyrene nanoparticles in different cell lines, *PLoS One 6*, e24438.

[132] dos Santos, T., Varela, J., Lynch, I., Salvati, A., and Dawson, K. A. (2011) Quantitative assessment of the comparative nanoparticle-uptake efficiency of a range of cell lines, *Small 7*, 3341-3349.

[133] Salvati, A., Aberg, C., dos Santos, T., Varela, J., Pinto, P., Lynch, I., and Dawson, K. A. (2011) Experimental and theoretical comparison of intracellular import of

polymeric nanoparticles and small molecules: toward models of uptake kinetics, *Nanomedicine 7*, 818-826.

[134] Lesniak, A., Campbell, A., Monopoli, M. P., Lynch, I., Salvati, A., and Dawson, K. A. (2010) Serum heat inactivation affects protein corona composition and nanoparticle uptake, *Biomaterials 31*, 9511-9518.

[135] Röcker, C., Pötzl, M., Zhang, F., Parak, W. J., and Nienhaus, G. U. (2009) A quantitative fluorescence study of protein monolayer formation on colloidal nanoparticles, *Nat. Nanotechnol. 4*, 577-580.

[136] Schottler, S., Klein, K., Landfester, K., and Mailander, V. (2016) Protein source and choice of anticoagulant decisively affect nanoparticle protein corona and cellular uptake, *Nanoscale 8*, 5526-5536.

[137] Green, R. J., Davies, M. C., Roberts, C. J., and Tendler, S. J. (1999) Competitive protein adsorption as observed by surface plasmon resonance, *Biomaterials 20*, 385-391.

[138] Kim, D., El-Shall, H., Dennis, D., and Morey, T. (2005) Interaction of PLGA nanoparticles with human blood constituents, *Colloids Surf., B 40*, 83-91.

[139] Song, H., Xu, Q., Zhu, Y., Zhu, S., Tang, H., Wang, Y., Ren, H., Zhao, P., Qi, Z., and Zhao, S. (2015) Serum adsorption, cellular internalization and consequent impact of cuprous oxide nanoparticles on uveal melanoma cells: implications for cancer therapy, *Nanomedicine (London, England) 10*, 3547-3562.

[140] Yu, S. M., Gonzalez-Moragas, L., Milla, M., Kolovou, A., Santarella-Mellwig, R., Schwab, Y., Laromaine, A., and Roig, A. (2016) Bio-identity and fate of albumin-coated SPIONs evaluated in cells and by the C. elegans model, *Acta Biomater. 43*, 348-357.

[141] Mirshafiee, V., Kim, R., Mahmoudi, M., and Kraft, M. L. (2016) The importance of selecting a proper biological milieu for protein corona analysis in vitro: Human plasma versus human serum, *Int. J. Biochem. Cell. Biol. 75*, 188-195.

[142] Laurent, S., Burtea, C., Thirifays, C., Rezaee, F., and Mahmoudi, M. (2013) Significance of cell "observer" and protein source in nanobiosciences, *J. Colloid Interface Sci. 392*, 431-445.

[143] Silva, A. M., Varela-Moreira, A., Pereira Gomes, C., Molinos, M., Leite, M., Almeida, M., Ribeiro, D., Schrader, M., Figueiredo, C., Barbosa, M., Goncalves, R., Almeida, C., Pego, A., Santos, S. G., and Gomez-Lazaro, M. (2015) Integrated Analysis of Biological Samples by Imaging Flow Cytometry, *Microsc. Microanal. 21 Suppl 5*, 95-96.

[144] Phanse, Y., Ramer-Tait, A. E., Friend, S. L., Carrillo-Conde, B., Lueth, P., Oster, C. J., Phillips, G. J., Narasimhan, B., Wannemuehler, M. J., and Bellaire, B. H.

(2012) Analyzing Cellular Internalization of Nanoparticles and Bacteria by Multi-spectral Imaging Flow Cytometry, *JoVE*, 3884.

Annex

Table S1- Albumin standards and respective RFU values. Average is obtained from two replicas. The blank value is subtracted from the average value of each standard.

[Protein] µg/ml	Average / RFU	Average - Blank / RFU
2000	0.973	0.898
1500	0.756	0.681
1000	0.503	0.428
750	0.398	0.323
500	0.285	0.209
250	0.172	0.096
125	0.116	0.040
Blank	0.076	

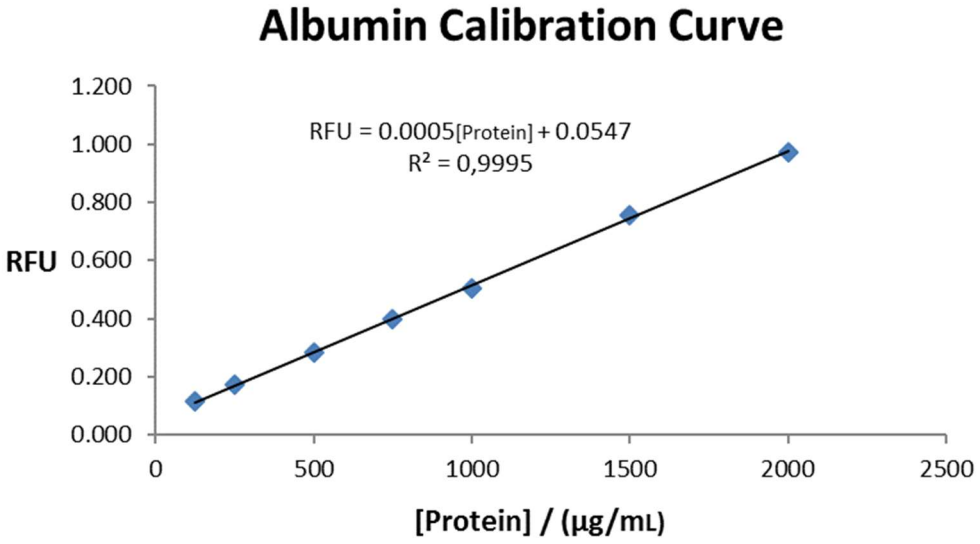

Figure S1 - Albumin calibration curve plotted with the results presented in Table 3.

Table S2- Measurements of fluorescence of FBS, PBF and HA serum, with a dilution factor of 1:10, and respective total protein content. This was a possible example on how to proceed with the quantification of protein content.

Serum	Replica 1 / RFU	Replica 2 / RFU	Replica 3 / RFU	Average / RFU	Average-blank / RFU	Total protein (µg/ml)
FBS	3.697	3.735	3.693	3.708	3.633	7156.27
PBF	3.351	3.350	3.376	3.359	3.284	6457.60
HA	1.874	1.878	1.680	1.811	1.735	3360.93

Knowing the total protein content of each serum, it was then possible to determine the % PBF and % HA providing the same protein content as 10% of FBS, through the following formula:

$$\frac{100\% \times Total\ protein\ content\ (FBS)}{Total\ protein\ content\ (PBF\ or\ HA)} = \%\ of\ PBF\ or\ \%\ of\ HA\ needed$$

$$\Leftrightarrow \frac{0.10 \times 7156.27}{6457.60} = 11.1\ \%$$

Table S3 - % values of serum in CM, obtained in this example with the results of Table S 2.

Serum	% in CM
FBS	10.0
PBF	11.1
HA	21.3

Three different solutions were prepared and then used to incubate the NPs before adding the mixture to the cells. It is also worth mentioning that every time a new stock of serum was used, the respective protein content was determined in order to assure maximum reproducibility.

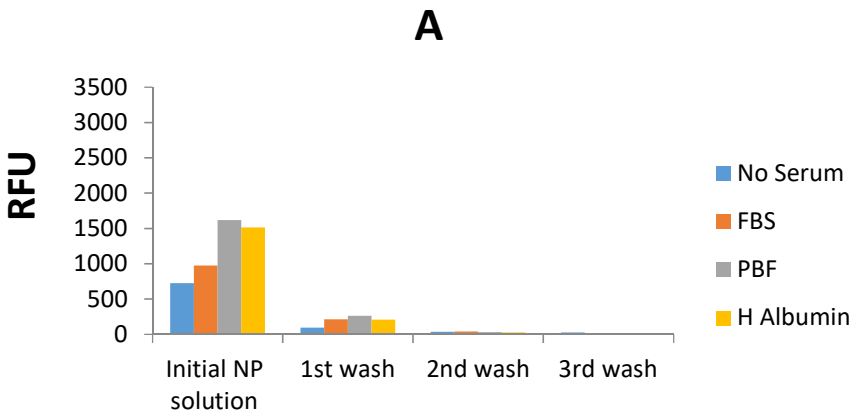
A
RFU
3500
3000
2500
2000
1500
1000
500
0
Initial NP solution
1st wash
2nd wash
3rd wash
No Serum
FBS
PBF
H Albumin

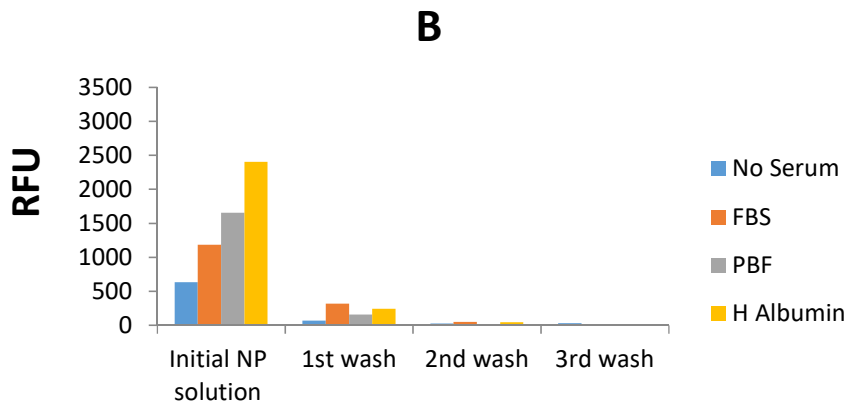
B
RFU
3500
3000
2500
2000
1500
1000
500
0
Initial NP solution
1st wash
2nd wash
3rd wash
No Serum
FBS
PBF
H Albumin

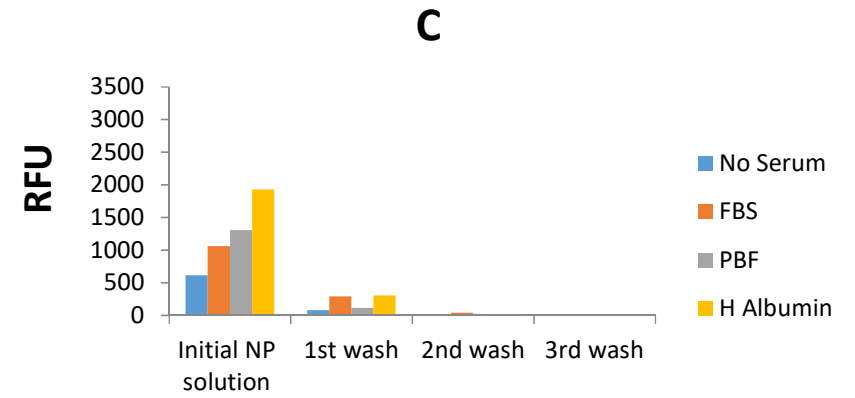
C
RFU
3500
3000
2500
2000
1500
1000
500
0
Initial NP solution
1st wash
2nd wash
3rd wash
No Serum
FBS
PBF
H Albumin

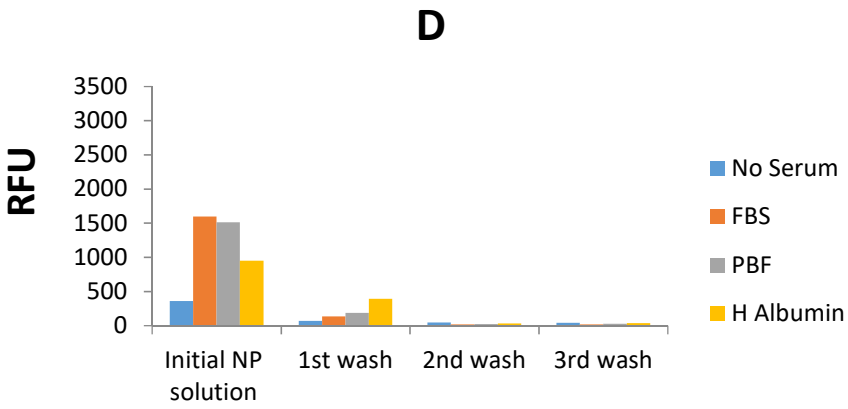
D
RFU
3500
3000
2500
2000
1500
1000
500
0
Initial NP solution
1st wash
2nd wash
3rd wash
No Serum
FBS
PBF
H Albumin

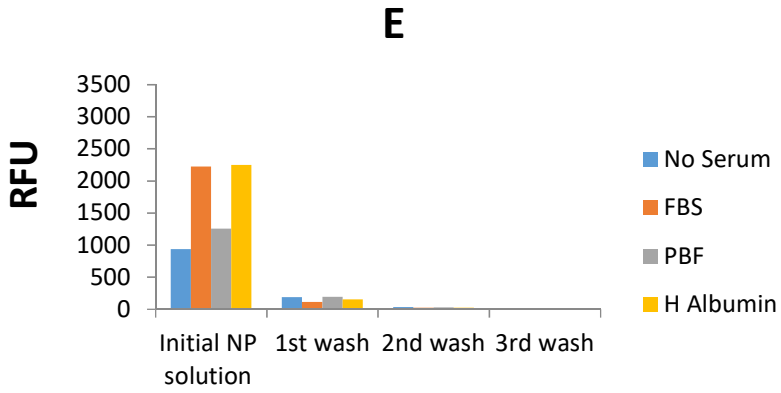
E
RFU
3500
3000
2500
2000
1500
1000
500
0
Initial NP solution
1st wash
2nd wash
3rd wash
No Serum
FBS
PBF
H Albumin

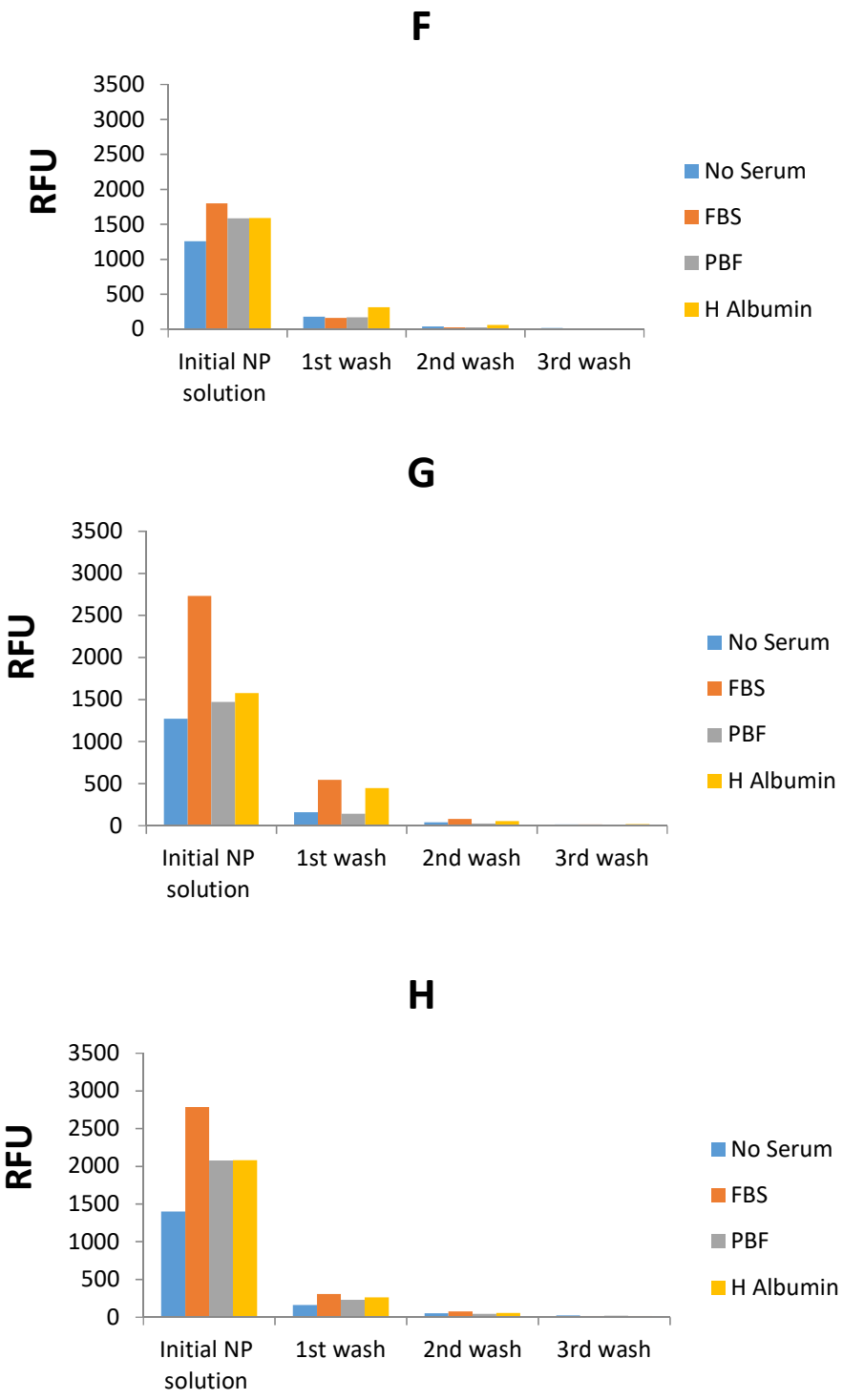

Figure S2 – Fluorescence intensity results of the 20, 100, 200 and 500 NP solution used to incubate cells and supplemented with different *sera*, before incubation and after three washes. (A-D) GP202 cells. (A) 20 NP solution, (B) 100 NP solution, (C) 200 NP solution, and (D) 500 NP solution. (E-H) MKN28 (CD44v6c -) cells, (E) 20 NP solution, (F) 100 NP solution, (G) 200 NP solution, and (H) 500 NP solution.

Table S4- Statistical report obtained in the analysis of the imaging flow cytometry results, in the IDEAS software.

Cell Line	Condition	NP Size	Cell Count	Cell # used in Median calculation	% of non-usable cells	Median
Hek293t	No Serum	40 nm	9626	1963	79.6	2.722
		500 nm	9670	2303	76.2	3.551
	FBS	40 nm	10160	4221	58.5	1.966
		500 nm	9552	3288	65.6	3.374
	PBF	40 nm	9659	2889	70.1	1.201
		500 nm	9578	2914	69.6	3.034
	HA	40 nm	9747	2800	71.3	2.068
		500 nm	9711	2626	73.0	3.255
HeLa	No Serum	40 nm	9762	3769	61.4	3.84
		500 nm	6834	3501	48.8	4.375
	FBS	40 nm	9648	3284	66.0	2.97
		500 nm	9668	3083	68.1	4.973
	PBF	40 nm	9636	3168	67.1	1.318
		500 nm	9817	3202	67.4	4.817
	HA	40 nm	9714	3817	60.7	3.478
		500 nm	9698	3327	65.7	4.604
GP202	No Serum	40 nm	9657	4990	48.3	2.588
		500 nm	9751	4833	50.4	2.622
	FBS	40 nm	9159	3501	61.8	2.519
		500 nm	9005	3781	58.0	2.996
	PBF	40 nm	9583	4339	54.7	1.855
		500 nm	9901	4604	53.5	3.336
	HA	40 nm	9855	4331	56.1	2.321
		500 nm	9936	4369	56.0	2.626
AGS	No Serum	40 nm	9617	4186	56.5	3
		500 nm	10059	4580	54.5	3.779
	FBS	40 nm	9780	4134	57.7	1.54
		500 nm	9850	3389	65.6	3.542
	PBF	40 nm	9858	3252	67.0	0.9137
		500 nm	9809	3457	64.8	3.544
	HA	40 nm	9732	3183	67.3	2.022
		500 nm	9858	3118	68.4	3.39
MKN28	No Serum	40 nm	9658	4662	51.7	1.831
		500 nm	6394	1019	84.1	1.969
	FBS	40 nm	9471	4256	55.1	1.043
		500 nm	9465	2858	69.8	2.398
	PBF	40 nm	7972	2278	71.4	0.4874
		500 nm	5983	423	92.9	1.395
	HA	40 nm	9717	4501	53.7	1.309
		500 nm	8211	1707	79.2	0.7611

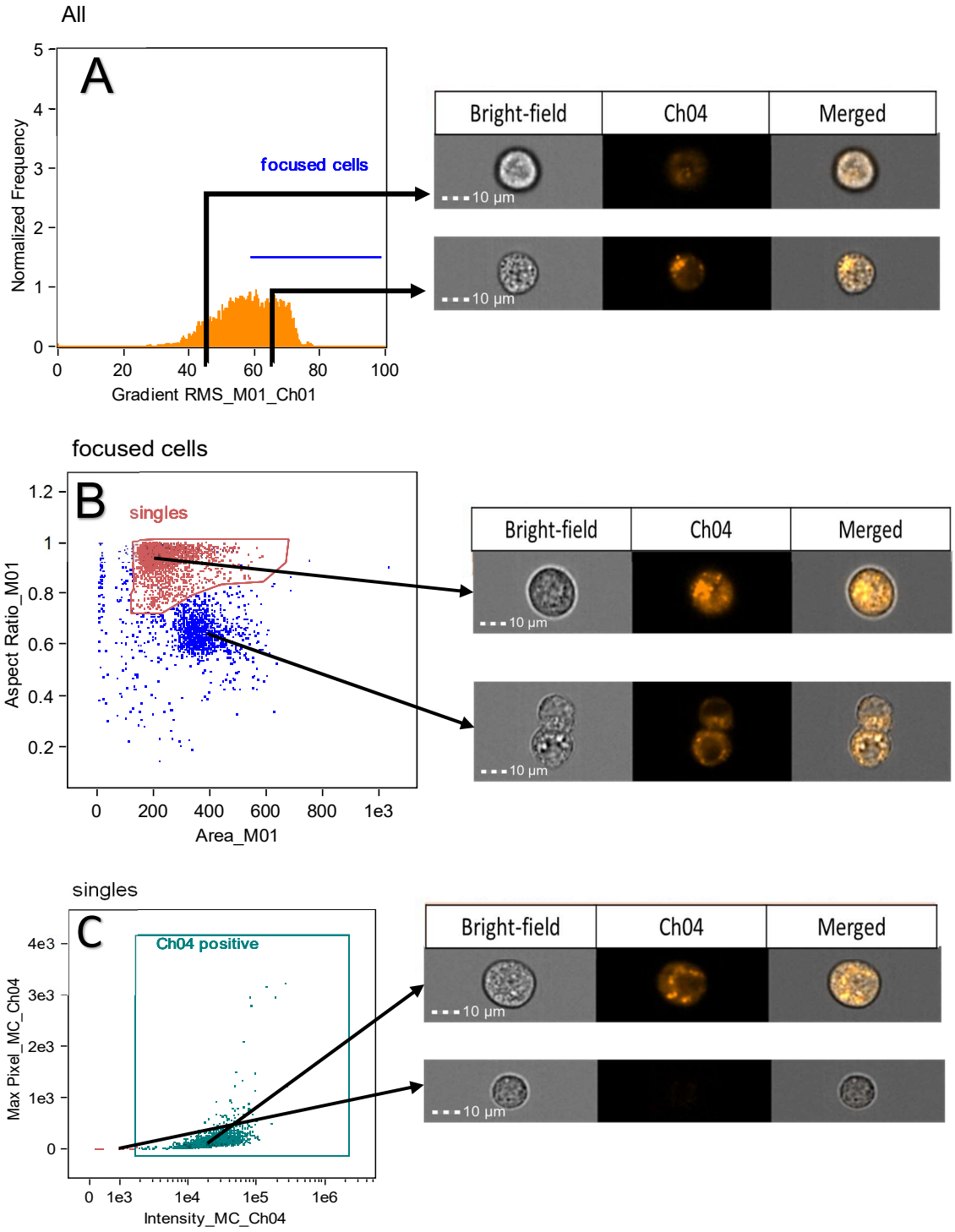
All
A
Normalized Frequency
Gradient RMS_M01_Ch01
focused cells
Bright-field
Ch04
Merged
10 µm
10 µm
focused cells
B
singles
Aspect Ratio_M01
Area_M01
Bright-field
Ch04
Merged
10 µm
10 µm
singles
C
Ch04 positive
Max Pixel_MC_Ch04
Intensity_MC_Ch04
Bright-field
Ch04
Merged
10 µm
10 µm

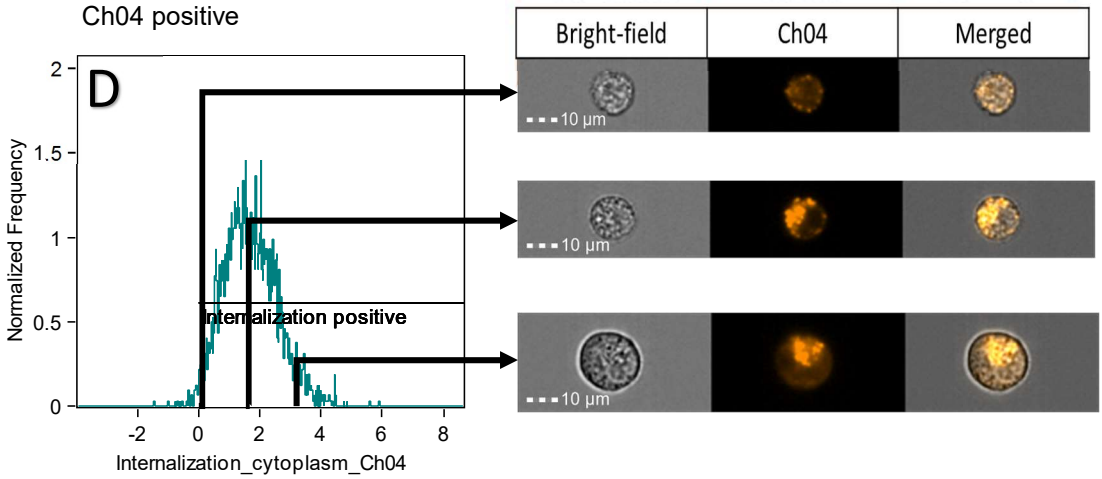

Figure S3 - Schematic exemplifying the usage of the internalization feature of Imagestream, in the uptake of 40 nm NPs, in serum free medium, by MKN28 cells. (A) Selection of focused cells area in the initial histogram. (B) Gating of the single cells, separating them from debris and double cells. (C) Gating of MKN28 cells positive for NPs, leaving the negative ones out of the gate. (D) Internalization score histogram, where the positions of the three different cells can be seen, with different scores of internalization. The work done on this sample was then used as the template for the remaining analysis of the rest of the samples

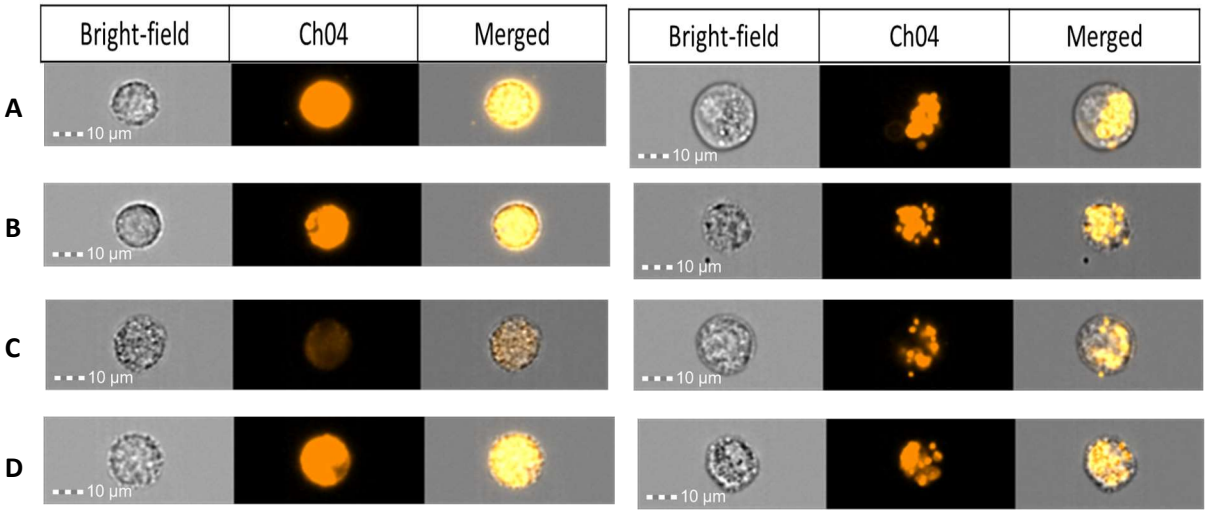

Figure S 4 - Comparison of the uptake of 40 nm NPs (left images) with the uptake of 500 nm NPs (right images), in HeLa cell line. (A) Uptake of NPs incubated in SFM. (B) Uptake of NPs incubated in media supplemented with FBS. (C) Uptake of NPs incubated in media supplemented with PBF. (D) Uptake of NPs incubated in media supplemented with HA.